

Lattice-stabilized CH_3 , C_2H_5 , NO_2 , and O^{1-} radicals in feldspar with different Al-Si order

IVAN PETROV

Institute of Mineralogy, University of Marburg, Hans-Meerwein-Straße, 35043 Marburg, Germany

ABSTRACT

Single crystals of feldspar with varying degrees of Al-Si order and from different petrogenetic areas were studied using electron paramagnetic resonance (EPR) spectroscopy. EPR spectra of lattice-stabilized CH_3 , C_2H_5 , and NO_2 free radicals could be detected in pegmatitic microcline and hyalophane. Spectra of this type were observed in microcline from pegmatites and granites of the Ukrainian Shield by Matyash et al. (1981, 1982), but the hydrocarbons were interpreted as HN_3^+ , and NO_2 as N^{2-} . Methyl and ethyl radicals at M positions in the feldspar structure are formed from methane and ethane after natural or artificial irradiation.

The CH_3 and NO_2 radicals in 34 microcline and hyalophane crystals and those reported by Matyash et al. (1981, 1982) show similar eigenvalues and direction cosines of the g and T tensors. The calculated spin densities in the NO_2 radical for temperatures between 295 and 30 K are $c_s^2 = 0.092\text{--}0.096$ and $c_{pz}^2 = 0.322\text{--}0.610$ on the N atom. In this temperature range the O-N-O angle varies between 129–138 and 130–140° for hyalophane and microcline, respectively.

Based on comparison of the direction cosines of the g tensor and T-T directions in the feldspar structure, five $\text{O}^{1-}/^{27}\text{Al}$ centers could be assigned to the bridges $\text{Al}_{\text{T}10}\text{-O}_{\text{A}1}^{\text{I-}}\text{-Al}_{\text{T}1\text{m}}$, $\text{Al}_{\text{T}10}\text{-O}_{\text{C}0}^{\text{I-}}\text{-Al}_{\text{T}2\text{m}}$, $\text{Al}_{\text{T}10}\text{-O}_{\text{B}0}^{\text{I-}}\text{-Al}_{\text{T}2\text{m}}$, $\text{Al}_{\text{T}1\text{m}}\text{-O}_{\text{Cm}}^{\text{I-}}\text{-Al}_{\text{T}20}$, and $\text{Al}_{\text{T}1\text{m}}\text{-O}_{\text{Dm}}^{\text{I-}}\text{-Al}_{\text{T}20}$ (violations of the rule of Loewenstein) in different samples and are designated as a_1' , c_0 , d_0 , c_m , and d_m , respectively. In albite one additional $\text{O}^{1-}/^{27}\text{Al} \times ^{23}\text{Na}$ center could be assigned to a $\text{Si}_{\text{T}10}\text{-O}_{\text{A}1}^{\text{I-}}\text{-Al}_{\text{T}1\text{m}}$ bridge with two adjacent quasi-equidistant Na atoms and is designated as a_1' . In feldspars with large M cations ($\text{M} = \text{K}, \text{Ba}$), independent of their degree of long-range Al-Si order, only a_1' and d_0 centers are formed, with a concentration ratio 3:1. In albite a_1' , c_0 , d_0 , c_m , and d_m centers with a concentration ratio 2:2:2:1:1 are present. After irradiation of ordered and disordered feldspars, $\text{O}^{1-}/^{27}\text{Al}$ centers could be created only in quasi-ordered domains of similar Al-Si order. Their total concentration is approximately the same in feldspars with large and small M cations. The short-range Al site occupancy in such domains indicated different ordering paths in feldspars with large and small M cations.

In the feldspar structure crystal defects, for example, $\text{O}^{1-}/^{27}\text{Al}$ centers and OH or H_2O may support the Al-Si exchange, whereas thermally stable Fe^{3+} substituting for Al at border tetrahedra between ordered and disordered domains can act as a stabilizer. With increasing total Fe_2O_3 content the concentration of $\text{O}^{1-}/^{27}\text{Al}$ centers decreases, the substitution of Fe^{3+} at tetrahedral positions increases, and the Al-Si exchange kinetics becomes slower.

INTRODUCTION

The type and concentration of crystal defects in natural minerals will certainly depend on the presence of specific ions in mineral-forming fluids, P , T , P_{O_2} , $P_{\text{H}_2\text{O}}$, etc., and small deviations in thermodynamic relationships during crystallization. Subsequent processes such as metasomatism, metamorphism, and natural irradiation can also influence these defects; thus the real structure of a mineral reflects its geological history. Crystal defects are central to the kinetics of transport in minerals and are essential in many geochemical processes, e.g., alteration of the

composition of minerals, homogenization of zoned crystals, changes in the degree of Al-Si order in aluminosilicates, etc. These crystal defects are inherently paramagnetic or become paramagnetic by natural or artificial irradiation; thus they are detectable by electron paramagnetic resonance (EPR). The study of impurity paramagnetic centers may give information about the crystallographical position (substitution at a structural site, interstitials, distribution of nonequivalent sites), valence and bonding state of trace elements, and data on more complex centers that can only be provided by other meth-

TABLE 1. Paramagnetic centers in alkali feldspar

Paramagnetic center	Notation/site	Degree of Al-Si order	T_m (K)	T_A (K)	t_A (h)	References
Thermally stable centers: Cations with d⁵ electron configuration						
Fe ³⁺ O ₄	T10	ordered	295	>1123	>200	a,b,c,d,e,f
Fe ³⁺ O ₄	T1 + T2	disordered	295	>1323	>3300	g
Fe ³⁺ O ₂ OH	T1	disordered	295	>1323	>1300	g
Fe ³⁺ O ₂ (OH) ₂	T1	disordered	15	>1273	>113	h
⁵⁵ Mn ²⁺	M	ordered + disordered	295	>1323	>3300	b,f,i,j
Iron oxides	—	ordered + disordered	295	>1323	>1	f,g,h,k
Thermally metastable centers: Free radicals						
Cations with unusual valence: d ¹ and p ¹ electron configuration						
Ti ³⁺	T10	ordered + disordered	(?)77	593	~2	l,m
[Pb-Pb] ³⁺	M-M	ordered	40	723	~2	h,r
Anions with unusual valence: p ⁵ electron configuration (O ¹⁻ /ΣM, and O ⁻¹ /ΣY, × ΣZ, centers)						
M = Si, M ²⁺ , n = 2	h(b _m)*, h(c _m), h(d _m)	ordered + disordered	5115	623	~3	h,l,m,n,s
Y = ²⁷ Al, n = 1	a _i	ordered	110	493	~3	m,n,o
Y = ²⁷ Al, n = 2	a _i ^o , c _o , d _o [*] , c _m , d _m	ordered + disordered	60	493	~3	l,m,n,o,p,s
Y = ²³ Na, n = 1	a _i (?)/M	ordered	(?)77	493	~2	l
Y = ²⁷ Al, n = 1;						
Z = ²³ Na, m = 2	a _i /T1m/M	ordered	60	553	~3	n
Y = ^{107,109} Ag ¹⁺ , n = 1	a _i (?)/M	ordered	(?)77	553	1.5	l
Y = ²⁰⁷ Pb ²⁺ , n = 1	c _m /M	ordered	(?)77	553	~2	l,m
BO _m ⁿ radicals						
SiO ₃ ⁻	e(m)	ordered + disordered	(?)77	598	~3	h,s
SiO ₃ ⁻ / ²⁷ Al	e(b _i)	ordered	295	653	0.3	l,o
PO ₃ ^{-**}	T2(?)	ordered	(?)77	(?)623	~3	q
NO ₂ †	M	ordered + disordered	70	873	0.3	l,o,s
Organic radicals						
C ₂ H ₅ ‡	M	ordered + disordered	295	573	0.3	l,o,s
CH ₃	M	ordered + disordered	295	573	0.3	l,o,s

Note: a = Höchli (1964), b = Marfunin and Michoulier (1966), c = Marfunin et al. (1967), d = Gaite and Michoulier (1970), e = Michoulier and Gaite (1972), f = Petrov et al. (1989a), g = Petrov and Hafner (1988), h = Petrov (1992), i = Matyash et al. (1981), j = Niebuhr et al. (1973), k = Petrov (1985), l = Marfunin and Bershov (1970), m = Speit and Lehmann (1976, 1982), n = Petrov et al. (1989b), o = Matyash et al. (1982), p = Joffe and Yanchevskaya (1968), q = Hofmeister and Rossman (1985), r = Petrov et al. (1993), s = this work.

* Interpreted as h(b_o) and b_o, respectively, by authors m.

** The PO₃⁻ signals were labeled as unknown by the authors.

† Interpreted as N²⁻ by authors i, o.

‡ Interpreted as NH₃⁺ by authors i, o.

ods with some difficulty. Thus, the study of many crystal-chemical, geochemical, and petrological phenomena is possible on an atomic scale.

In the past three decades 20 paramagnetic centers have been detected by EPR measurements of oriented single crystals, and their positions in the structure of natural feldspars were determined (Table 1). Their spectra can be observed between 4.2 and 295 K, showing different characteristic temperatures T_m , where the intensities of the EPR lines are at a maximum. T_m can depend on center concentration and the degree of Al-Si order. Only the 3d⁵ impurity paramagnetic centers, Fe³⁺ and Mn²⁺, are bonded covalently to the diamagnetic O²⁻ ligands. They are thermally stable and cannot be destroyed by heating at annihilation temperatures T_A above 873 K. Thermally metastable paramagnetic centers have $T_A \leq 873$ K for various annihilation times t_A above 873 K. Thermally metastable paramagnetic centers have $T_A \leq 873$ K for various annihilation times t_A and can be reactivated after subsequent natural or artificial irradiation. Therefore, systematic studies of T_A and concentration of these centers can recognize thermodynamic and radiologic gradients in geological profiles. These paramagnetic centers can be summarized into four main groups: cations and anions

with unusual valence, BO_mⁿ radicals, and organic radicals (Table 1).

In ordered alkali feldspars, Fe³⁺ occupies the T10 position (Höchli, 1964; Marfunin and Michoulier, 1966; Marfunin et al., 1967; Gaite and Michoulier, 1970; Michoulier and Gaite, 1972; Petrov et al., 1989a). In disordered ones it is found at the T1 and T2 positions, as well as in tetrahedra of type TO₃OH (Petrov and Hafner, 1988). In hydrocarbon-bearing hyalophane, FeO₂(OH)₂ centers occur after X-ray or γ irradiation (Petrov, 1992). Three lattice positions of Fe³⁺ in the structure of intermediate plagioclase are still under discussion (Marfunin and Michoulier, 1966; Marfunin et al., 1967; Gaite and Michoulier, 1970; Niebuhr et al., 1973; Scala et al., 1978; Petrov, 1992). Submicroscopic iron oxide particles (<10 nm) with hematite-like structures were found in albite, microcline, adularia, orthoclase, and sanidine (Petrov, 1985, 1992; Petrov and Hafner, 1988; Petrov et al., 1989a).

Mn²⁺ was detected in oligoclase (Marfunin and Michoulier, 1966; Matyash et al., 1981), anorthite (Niebuhr et al., 1973), albite (Petrov et al., 1989a), and sanidine after heat treatment at 1323 during $t_A = 3300$ h (Petrov, unpublished data). The Ti³⁺ electron center (Ti⁴⁺ + e)

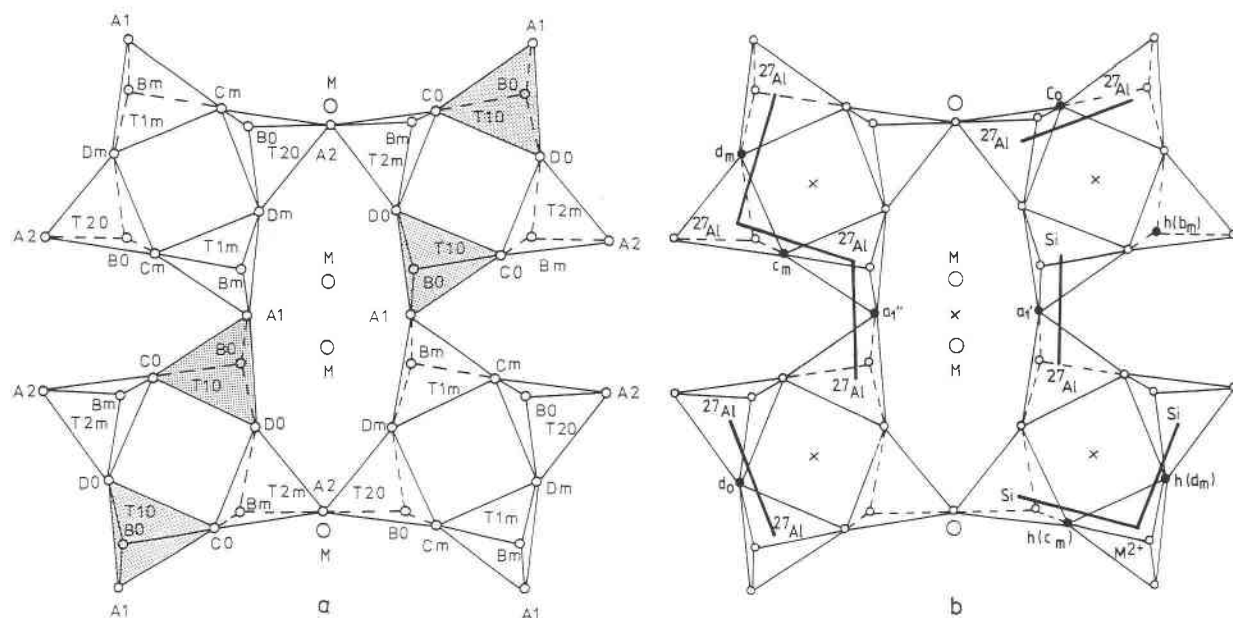


Fig. 1. Projection of the crystal structure of feldspar on the (201) plane. The projections of **a** and **b** are identical. In **a**, the atomic positions of Na, Al, Si, and O are labeled using the notation of Megaw (1956). The T10 tetrahedra of the regular Al position in ordered feldspar are shaded.

In **b**, the most probable assignments of the $O^{1-}/^{27}Al$ centers are marked by heavy lines. These were obtained from the g_{zz} eigenvectors of the mean positions of the centers, which are assumed to be about parallel to the direction of the line connecting the two effective T positions. The g_{zz} eigenvectors of the $O^{1-}/$

(Si, M^{2+}) centers are approximately parallel to the T-O direction. The distinct $O^{1-}/^{27}Al$ centers, a' , c_0 , d_0 , c_m , and d_m , are assigned to the bridges $Al_{T10}-O_{A1}^- - Al_{T1m}$, $Al_{T10}-O_{C0}^- - Al_{T2m}$, $Al_{T10}-O_{B0}^- - Al_{T2m}$, $Al_{T1m}-O_{Cm}^- - Al_{T20}$, and $Al_{T1m}-O_{Dm}^- - Al_{T20}$, respectively.

The $O^{1-}/^{27}Al \times ^{23}Na$ center, a' , is assigned to a $Si_{T10}-O_{A1}^- - Al_{T1m}$ bridge that possesses two adjacent quasi-equidistant Na atoms. The distinct $O^{1-}/(Si, M^{2+})$ centers, $h(b_m)$, $h(c_m)$, and $h(d_m)$, are assigned to O^{1-} at Bm, Cm, and Dm, with a bivalent cation, e.g., Mg^{2+} , substituted for one of the Si atoms at the two adjacent T1m and T20 or T2m tetrahedra.

was detected in various ordered and disordered feldspars (Marfunin and Bershov, 1970; Speit and Lehmann, 1982). The $[Pb-Pb]^{3+}$ dimeric center ($[Pb-Pb]^{4+} + e$) was discovered in amazonite-type microcline (Petrov et al., 1993). Distinct O^{1-} hole centers were observed in different ordered and disordered feldspars (Joffe and Yanchevskaya, 1968; Marfunin and Bershov, 1970; Speit and Lehmann, 1976, 1982; Matyash et al., 1981, 1982; Petrov et al., 1989b). They can be described by the formula

$$O^{1-} / \left[\sum_{i=1}^n Y_i \times \sum_{j=1}^m Z_j \times \dots \right] \text{ and } O^{1-} / \left[\sum_{i=1}^n M_i \right] \quad (1)$$

where Y_i and Z_j are adjacent nuclei with $I > 0$, giving a hyperfine structure (HFS) and M_i adjacent nuclei with $I = 0$, without HFS. In feldspar $Y_i = ^{27}Al, ^{23}Na, ^{107,109}Ag, ^{207}Pb$, $Z_j = ^{23}Na$, and $M =$ unidentified cation, e.g., Si^{4+}, Mg^{2+} (Petrov et al., 1989b). Centers with $Y_i = ^{27}Al$, $n = 2$, (i.e., Al-O $^{1-}$ -Al bridges) cause a violation of the principle of Loewenstein (1954). The notation a_1, b_0, c_0 , etc., describes O^{1-} centers created at A1, B0, C0, etc., O positions in the feldspar structure (Fig. 1).

O^{2-} vacancies at Si tetrahedra with one captured electron (SiO_3^- radical) are similar to the E'_1 centers in quartz. PO_3^- electron centers were formed by substitution of P^{5+}

for Si^{4+} with an O vacancy and one captured electron in the complex.

EPR spectra of the free radicals NO_2 , CH_3 , and C_2H_5 were observed first by Matyash et al. (1981, 1982) in pegmatitic microcline from the Ukrainian Shield, but the NO_2 centers were interpreted as N^{2-} at D_m O positions ($Si-N^{2-}-Si$) and the hydrocarbon centers as NH_3^+ .

Natural fluids of the system C-O-H-N are important because of their geochemical significance. During crystallization, small parts of N- and hydrocarbon-bearing fluids can be trapped in the host crystal. Intracrystalline fluid inclusions of this composition have been investigated by analytical methods and Raman spectroscopy mainly in quartz, but only slightly in feldspar. However, information on the substitution of N and hydrocarbons in minerals is rare; their substitution in the structure of feldspar has not been reported. In the present study, the substitution of NO_2 , CH_4 , and C_2H_6 in microcline and hyalophane is discussed, and new data on the distribution of Al-O $^{1-}$ -Al fragments in the structure of feldspars with large and small M cations are reported.

EPR SPECTRA OF FREE RADICALS

Generally, free radicals in minerals represent ions or segments of molecules containing one unpaired spin,

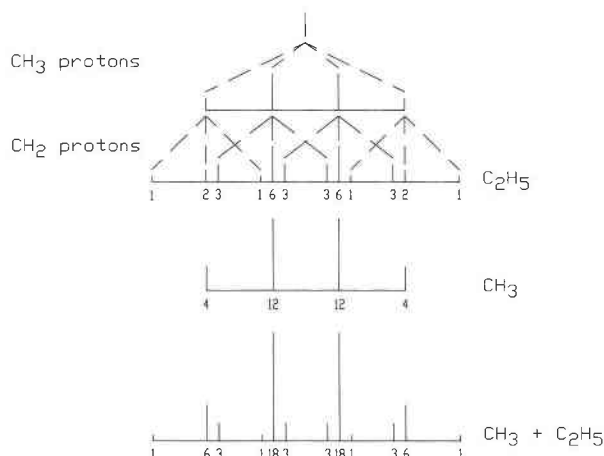


Fig. 2. Hyperfine structure patterns of methyl and ethyl radicals in feldspar.

thereby trapping or losing an electron. They do not occur as isolated groups because of the existence of a free valency but are stabilized by the crystal lattice. Irradiation-induced, thermally metastable paramagnetic centers in feldspar with annihilation temperatures $T_A \leq 873$ K (cf. Table 1) match these criteria.

The EPR spectrum of such a system consisting of one electron with spin $S = 1/2$ and n nuclei of spin I_i may be described by the spin Hamiltonian

$$\mathcal{H} = \beta \mathbf{B} \mathbf{g} \mathbf{S} + \sum_{i=1}^n \mathbf{S} \mathbf{A}_i \mathbf{I}_i \quad (2)$$

where β is the Bohr magneton, \mathbf{S} and \mathbf{I} are the electron and nucleus operators, respectively, \mathbf{g} and \mathbf{A} are the spectroscopic splitting factor and HFS tensors, respectively, and \mathbf{B} is the Zeeman field vector. Terms of the nuclear Zeeman energy and the nuclear quadrupole energy are omitted from Equation 2, since they are small.

In general, HFS tensor components may be written as sums:

$$A_{ii} = A_{\text{iso}} + T_{ii} \quad (3)$$

where A_{iso} is the isotropic hyperfine interaction (HFI) or Fermi contact interaction, and T_{ii} ($i = x, y, z$) are the principal components of the traceless dipole-dipole or anisotropic interaction tensor. Consequently, the HFS data may be analyzed with the aid of the expressions

$$A_{\text{iso}} = 8/3 g \beta g_n \beta_n |\Psi_{ns}(O)|^2 |c_s|^2 \quad (4)$$

and

$$T_{zz} = 4/5 g \beta g_n \beta_n \langle r^{-3} \rangle_{np} |c_p|^2 \quad (5)$$

where s and p relate to the central atom orbitals, and the parameters c_s^2 and c_p^2 represent the fraction of unpaired electron spin density at the central atom s and p orbitals, respectively.

Organic radicals

For most organic free radicals, since the orbital angular momentum is quenched, and \mathbf{g} has an almost isotropic value close to $g_e = 2.0023$, the value of the free electron,

the difference $g_{ii} - g_e = \Delta_{gii}$ ($i = x, y, z$) is small. Therefore, for an unambiguous identification of organic free radicals their HFS patterns are important. The number and the intensity ratio of HFS components give information about the radical structure. If the radical is observed in solution, the anisotropic contributions T_{ii} to the HFI between \mathbf{S} and \mathbf{I} are generally averaged to zero. Thus the HFS spectra of most organic radicals in fluid media can be interpreted simply by the third term, $\mathbf{S} \mathbf{A}_i \mathbf{I}_i$, of Equation 2. For organic paramagnetic centers examined in fixed orientations to \mathbf{B} , as in a single crystal, in which the effect of the coupling between electron spin and orbital angular momentum can be observed, anisotropy in \mathbf{g} , as well as A_{iso} and T_{ii} from Equation 3 must be taken into account. For intermediate situations, e.g., for radicals trapped in polycrystalline matrices, which occupy sites with random orientations with respect to \mathbf{B} , A_{iso} and T_{ii} components may be separated only in favorable cases. In many systems A_{iso} is much greater in magnitude than T_{ii} , and so the latter cause only line broadening.

According to Equation 3 a Fermi contact interaction A_{iso} can be expected only for radicals with $c_s^2 > 0$. But most organic radicals are π radicals, with their unpaired electron localized in an orbital without an s character. The unpaired electron in the CH_3 radical occupies a $2p_{zr}$ orbital in the carbon sp^2 hybrid orbital. The $2p_{zr}$ orbital is oriented perpendicular to the $>\text{C-H}$ bond. Because of the π - σ spin polarization, a contact interaction between the unpaired electron and the three equivalent protons takes place. Theoretical calculations suggest that the unpaired $2p_{zr}$ electron induces a negative spin density of about $c_s^2 = -0.05$ in the H $1s$, orbital, corresponding to a HF coupling constant A_{iso} of -56 up to -70 MHz (e.g., Carrington and McLachlan, 1967). Experimental data are in good agreement with these values (Jen et al., 1968; Fessenden and Schuler, 1963; Bersohn and Baird, 1966; Ayscough, 1967; Carrington and McLachlan, 1967; Wertz and Bolton, 1972).

In general, if the unpaired electron interacts with an arbitrary number of sets of equivalent protons, the number of equidistant HFS components N_{HFS} will be given by

$$N_{\text{HFS}} = \prod_i (2n_i I_i + 1) \quad (6)$$

where n_i is the number of equivalent nuclei with spin I_i , and \prod_i indicates a product over all values of i . Sets of equivalent nuclei can be treated by considering that they interact as one nucleus with a nuclear spin equal to the sum of all the nuclear spins in the equivalent set. Thus, if there are n equivalent nuclei of spin I , the HFI between \mathbf{S} and \mathbf{I} in the second term of Equation 2 leads to an EPR spectrum that consists of $N_{\text{HFS}} = (2nI + 1)$ lines. Their intensities are proportional to the coefficients of the binomial expansion of $(1 + x)^n$. The three equivalent protons ($I = 1/2$, natural abundance 99.98%) of the methyl radical lead to a multiple that consists of $N_{\text{HFS}} = 4$ lines with an intensity ratio of 1:3:3:1 (Fig. 2). The portion of the ^{12}C nucleus with $I = 0$ is 98.9%; thus no additional HFS appears. The remaining 1.1% belongs to the ^{13}C nuclei with $I = 1/2$, which can give an additional HFS. How-

ever, it is too weak to be observed in spectra of natural minerals.

If there exist two sets of n_α and n_β equivalent protons, then the maximum possible N_{HFS} in the spectrum will be given by $(2n_\alpha I_\alpha + 1)(2n_\beta I_\beta + 1)$. For the ethyl radical with two equivalent CH_2 and three equivalent CH_3 protons ($I_\alpha = I_\beta$), 12 lines with an intensity ratio of 1:2:3:1:6:3:3:6:1:3:2:1 are expected. As shown in Figure 2, the HFI with two sets of protons with different HF splittings gives spectra rich in line components. More complex HFS patterns and intensity ratios were produced by superposition of such spectra of distinct centers so that an unambiguous identification of the centers is difficult. The overlapping of ethyl and methyl spectra in feldspar is schematically shown in Figure 2.

In the usual notation the C atom holding the unpaired electron is designated as α carbon, and the protons bonded to it are labeled α protons. The C atoms bonded to the α carbon are designated as β carbon atoms, and the protons bonded to the β carbon atoms are called β protons. In the ethyl radical CH_2CH_3 , the unpaired electron is localized in the $2p_{z\alpha}$ orbital of the $-\text{CH}_2$ group. Analogous to the methyl radical, a negative spin density in the $1s_\alpha$ orbital of the ethylene α protons is induced by the π - σ spin polarization, corresponding to $A_{1s_\alpha}^\alpha \approx -63$ MHz (Fessenden and Schuler, 1963; Bersohn and Baird, 1966; Ayscough, 1967; Carrington and McLachlan, 1967; Wertz and Bolton, 1972). The β methyl protons lie in a plane parallel to the axis of the $2p_z$ orbital of the unpaired electron, perpendicular to the C-C bond. The unpaired electron is delocalized into the β proton $1s_\beta$ orbital by a hyperconjugative mechanism, the resulting positive spin density is $A_{1s_\beta}^\beta \approx 78$ MHz.

Theory and experiment indicate that in radicals of this type the β hydrogen nuclei have approximately isotropic HFI. However, the α hydrogen nuclei will also experience an anisotropic HFI of the same order of magnitude as the isotropic HFI, whereas the HF anisotropy experienced by the β hydrogen atoms will be considerably smaller (e.g., Ayscough, 1967; Wertz and Bolton, 1972). In crystalline matrices the effect of the anisotropic HFI with the α hydrogen atoms will depend on the rotational freedom of the radical, e.g., the possibility of cancellation between two such α hydrogen atoms, local disorder around the radical site, etc. These effects can lead to increasing line width and a change in line shape. In polycrystalline matrices with a random orientation of T with respect to B, this anisotropy will produce a broadening of the lines, which may range from an obliteration of fine details of the spectrum to extreme broadening, so that the spectrum may appear as a single broad, weak (or even undetectable) line.

Inorganic radicals

As is the case for organic radicals, the values of T_{ii} and N_{HFS} in Equations 3 and 6, respectively, can provide the major clues in the identification of most inorganic radicals. However, the appearance of HFS is not sufficient to provide a positive identification. Paramagnetic centers as

N , NO_2 , NO_2^- , NO_3 , and NO_3^- , which contain a N atom, are characterized by $N_{\text{HFS}} = 3$. However, assignment to specific radicals requires a knowledge of the theoretical predictions of the structure and orbital sequence of each radical; in addition, one requires information from studies of these radicals in other host matrices. In various host matrices, NO_2 exhibits a ^{14}N HFI with little anisotropy, and $A_{\text{iso}} \geq 150$ MHz. The small anisotropy arises from the fact that NO_2 is usually rotating around its two-fold axis, even in a solid. NO_2 fixed in a host crystal exhibits considerable anisotropy. The large A_{iso} arises from the fact that the unpaired electron is located primarily in a nonbonding sp^3 orbital of N.

The NO_2 radical has 17 valence electrons with a ground-state electron configuration $(3b_2)^2(4a_1)^1$ and is predicted to have a bent structure with an O-N-O angle of about 134° (Ayscough, 1967; Atkins and Symons, 1967; Wertz and Bolton, 1972; Gimarc, 1979). Excitation of an electron from the lower $3b_2$ level to $(3b_2)^1(4a_1)^2$ makes this excited state of NO_2 more strongly bent (121°).

For such radicals, which have C_{2v} symmetry, the unpaired electron is in the antibonding $4a_1$ orbital, which is a mixture of s and p_z central atom orbitals and a symmetry-adapted linear combination of O 2s and 2p orbitals (e.g., Carrington and McLachlan, 1967). The general form of this orbital can be represented as

$$\Psi(4a_1) = c_s \psi_N(2s) + c_p \psi_N(2p_z) + c_o \psi_o \quad (7)$$

where ψ_N is the central atom orbital, ψ_o is a linear combination of O 2s and 2p orbitals, and $c_s^2 + c_{pz}^2 + c_o^2 = 1$.

For the NO_2 radical the eigenvector g_{xx} is perpendicular to the plane of the radical; the eigenvector g_{yy} is directed along the O-O direction, and g_{zz} bisects the O-N-O angle (Atkins and Symons, 1967; Carrington and McLachlan, 1967). The constants of the isotropic HFI and the components of the tensor of dipole-dipole HFI may be written as $A_{\text{iso}} = \sum A_{ii}/3$ and $T_{ii} = A_{ii} - A_{\text{iso}}$, respectively. Spin densities (s and p contribution) on the N atom are defined as $c_s^2 = A_{\text{iso}}/A_{\text{iso}}^*$, $c_{pz}^2 = T_{zz}/T^*$, where $^{14}A_{\text{iso}}^* = 1811$ MHz and $^{14}T^* = 55.52$ MHz are the constants of the isotropic and anisotropic HFI for a free N atom (Morton and Preston, 1978). From the calculated values of c_s^2 and c_{pz}^2 , the p to s hybridization ratio $\lambda^2 = c_{pz}^2/c_s^2$ can be determined for which the bond angle is given by

$$\rho = 2 \cos^{-1}(\lambda^2 + 2)^{-1/2}. \quad (8)$$

O^{1-} centers from Equation 1 with $Y_i = ^{27}\text{Al}$ and $n = 2$, described in detail in Petrov et al. (1989b), can be identified by its characteristic spectrum of $N_{\text{HFS}} = 11$, exhibiting line intensities according to the approximate ratio 1:2:3:4:5:6:5:4:3:2:1. A HFS pattern of this type is due to the interaction of an unpaired electron ($S = 1/2$) with two adjacent Al nuclei ($I = 3/2$, natural abundance of ^{27}Al 100%), which are separated from the hole center by about the same distance.

SAMPLES

The investigated crystals of hydrocarbon-bearing microcline and hyalophane (a monoclinic barium potassium

TABLE 2. Microprobe analyses of microcline and hyalophane

	Microcline	Hyalophane
SiO ₂	64.86	49.42
Al ₂ O ₃	19.07	21.82
BaO	nd	21.69
K ₂ O	11.27	5.68
Na ₂ O	3.58	1.55
CaO	nd	0.03
MgO	nd	0.01
FeO	0.02	0.03
SrO	nd	nd
MnO	nd	nd
NiO	0.02	nd
TiO ₂	nd	nd
Cr ₂ O ₃	0.01	nd
Total	98.83	100.25

Note: microprobe analyses by J.M. Claude, Université de Nancy. Analyses are given in weight percentages.

feldspar) were from Hagendorf pegmatite, Oberpfalz, Germany, and pegmatitic rocks of Bosovaca, Bosnia, respectively. The samples of hyalophane were fragments from the same larger crystals used in Beran et al. (1992). Chemical analyses of microcline and hyalophane are given in Table 2. No phases other than sodium feldspar and potassium feldspar were revealed by X-ray phase analyses of microcline. The sanidine samples (Or₆₉₋₈₂) were fragments of megacrystals from different localities (Volkesfeld, Wehr, Niederzißen, Essinger Maare, Rieden II) from leucite phonolite tuffs of the Eifel volcanic complex, Germany, described in Bertelmann et al. (1985) and in Petrov and Hafner (1988). The orthoclase crystals were Fe-rich samples from Madagascar. Crystals of adularia (Or_{91±0.3} Ab_{7.8±0.2} Cn_{1.2±0.1}) from Hybin pegmatite of the Kola peninsula were fragments from the larger crystal no. 1481/D, studied by Borutskyi et al. (1984). The albite samples from Amelia Court House, Virginia, U.S.A., were fragments of the same megacrystals as used by Petrov et al. (1989a, 1989b). Sanidine, hyalophane, orthoclase, adularia, and albite crystals were optically transparent, quite homogenous, and of gem quality.

The volumes of 87 single-crystal fragments cut for EPR experiments were about 1 mm³. The samples are {001} and {010} cleavage fragments spalled from larger crystals. Thin sections of the crystals were inspected optically for identification of the crystallographic axes; no inclusions or cracks were observed.

EXPERIMENTAL DETAILS

EPR spectra of single crystals were recorded on commercial X-band (between 4.2 and 295 K) and Q-band (at 295 K) spectrometers; details are described in Petrov and Hafner (1988). The applied magnetic field *B* for each recorded spectrum was calibrated by simultaneous measurement of *B* using a B-H15 field controller. The single crystals were aligned on a goniometer in the cavity of the spectrometer. They were rotated at different temperatures within the cryostat in the orthogonal laboratory system X⁰, Y⁰, Z⁰. Their relation to the crystallographic axes has been reported earlier (Petrov et al., 1989b). Spectra were recorded every 10°; over critical ranges spectra were re-

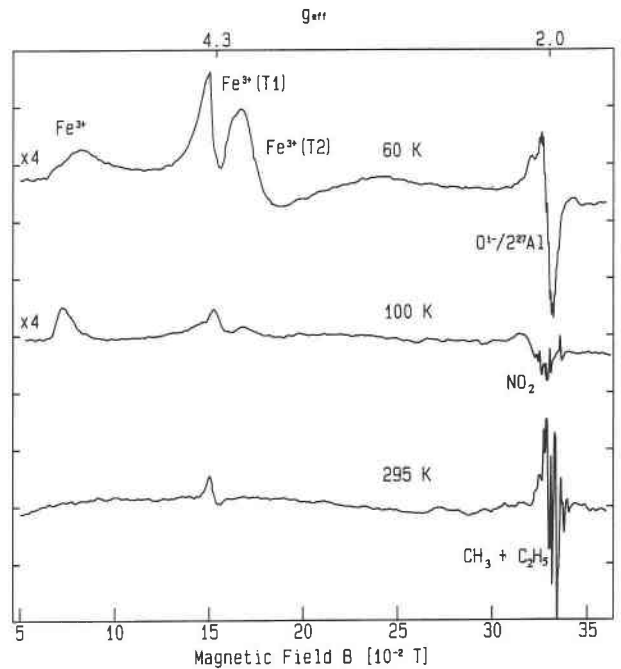


Fig. 3. EPR spectra of hyalophane recorded at different T_m . $T_m = 60$ K: γ irradiated, rotation $+a \parallel +Z^0$, $+c^* \parallel +X^0$, $\theta = 2^\circ$, $m = 9.2431$ GHz. $T_m = 100$ K: natural, rotation $+a \parallel +Z^0$, $+c^* \parallel +X^0$, $\theta = 104^\circ$, $m = 9.2428$ GHz. $T_m = 295$ K: γ irradiated, rotation $+b \parallel +Z^0$, $+a \parallel +X^0$, $\theta = 30^\circ$, $m = 9.5253$ GHz.

corded every 1–5°. The spin Hamiltonian parameters and direction cosines were obtained by matrix diagonalization.

Annihilation temperatures T_A of the paramagnetic centers were determined by stepwise annealing of the hydrocarbon-bearing microcline and hyalophane crystals in air. The annealing times at each temperature step were $t_A = 20$ min. These conditions are the same as those of Matyash et al. (1981, 1982) and were chosen for a better correlation with their data. To create paramagnetic centers or to increase their concentration up to saturation, the crystals were exposed to X-ray or γ irradiation (⁶⁰Co source) up to about 2×10^6 Gray. To avoid surface effects for heat treatments and irradiation experiments, only single crystals were used.

RESULTS

In the investigated natural and irradiated single crystals of feldspar, thermally stable Fe³⁺ and Mn²⁺ centers and distinct metastable paramagnetic centers of the groups B, C, and D from Table 1, with different values of T_m and T_A , could be detected.

In natural hyalophane no EPR spectra of hydrocarbon radicals can be detected, neither in the temperature range between 4.2 and 295 K in the X band nor at 295 K in the Q band. In the region of $g = 2$, spectra of the NO₂ radical can be observed between 20 and 295 K, with $T_m \approx 70$ K in the X band and at 295 K in the Q band. After X-ray and γ irradiation, the colorless crystals of heat-treated sanidine and thermally untreated hyalophane be-

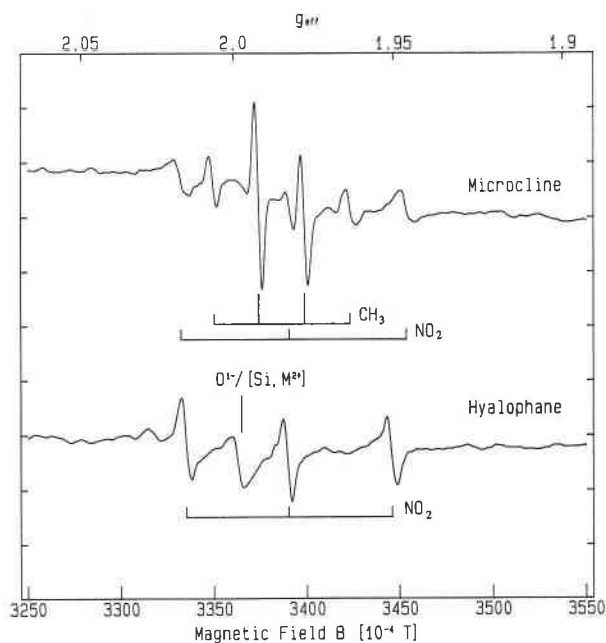


Fig. 4. EPR spectra of natural microcline and hyalophane. The spectrum of microcline consists of a superposition of the spectra of CH_3 , C_2H_5 (not resolved), and NO_2 radicals, rotation $+c^* \parallel +Z^0$, $+a \parallel +X^0$, $\theta = 90^\circ$, $m = 9.4965$ GHz, $T = 295$ K. In natural hyalophane, only spectra of NO_2 radicals and $h(b_m)$ centers could be observed, rotation $+a \parallel +Z^0$, $+c^* \parallel +X^0$, $\theta = 175^\circ$, $m = 9.4071$, $T = 295$ K.

came reddish brown. The color is produced by a'_1 and d_s centers; their spectra could be observed between 5 and 220 K, with $T_m \approx 60$ K, like those in albite (Petrov et al., 1989b). In the irradiated hyalophane, spectra of methyl and ethyl radicals can be observed at 295 K. Centers of type $h(b_m)$ can be detected in the whole temperature range between 4.2 and 295 K, with $T_m \approx 5$ K. In Figure 3 spectra of irradiated hyalophane, recorded at different values of T_m , are plotted. The broad signals or groups of signals in the region of $g \approx 4$ and $g \approx 9$ are caused by Fe^{3+} at T1 and T2 positions in monoclinic hyalophane, like those observed in sanidine (Petrov and Hafner, 1988).

In microcline from Hagendorf pegmatite a superposition of the spectra of the thermal metastable centers CH_3 , C_2H_5 , NO_2 , a'_1 , $h(c_m)$, and $e(m)$ are observable before or after artificial irradiation. In contrast to hyalophane, no Fe^{3+} signals can be found in any of the natural or irradiated hydrocarbon-bearing microcline crystals. Spectra of this type were reported first by Matyash et al. (1981, 1982) in microcline from granites and pegmatites from Ukrainian Shield, but the superposed spectra of CH_3 and C_2H_5 radicals were assigned to a NH_4^+ cation radical at the M site and those of the NO_2 radical to N^{2-} at D_m O positions in the feldspar structure.

Organic radicals

CH_3 center. The four prominent lines in the spectrum of microcline shown in Figure 4 are approximately equally spaced, and they obviously form the quartet with the

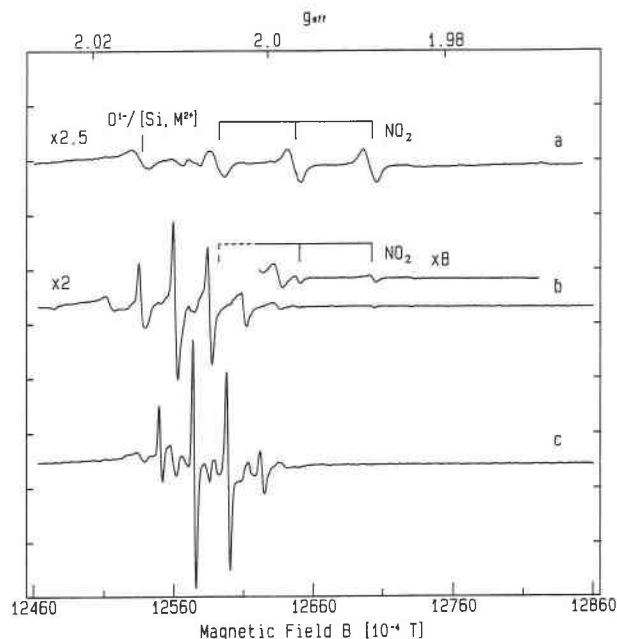


Fig. 5. EPR spectra of hyalophane: (a) natural, (b) and (c) irradiated with a γ dose of 2×10^6 Gray. In spectrum a rotation $+a \parallel +Z^0$, $+c^* \parallel +X^0$, $\theta = 163^\circ$, $m = 35.354$ GHz. In b same experimental conditions as for a. In c rotation $+c^* \parallel +Z^0$, $+a \parallel +X^0$, $\theta = 90^\circ$, $m = 35.361$ GHz, $T = 295$ K. Irradiation caused a decrease in the line intensity of the NO_2 spectrum (cf. spectra a and b).

intensity ratio 1:3:3:1, as expected for the methyl radical (cf. Fig. 2). This quartet can be observed in the spectrum of natural microcline but in hyalophane only after X-ray or γ irradiation (Fig. 5, spectra b and c). The HF tensor \mathbf{A} of the CH_3 center exhibits a small anisotropy; its average value is $A_{\text{iso}} = -71$ MHz for microcline and hyalophane. The individual peak to peak line widths, ΔB_{pp} , are the same in both minerals. For different crystal orientations with respect to \mathbf{B} , ΔB_{pp} is anisotropic and varies between $\Delta B_{pp}^l = 1.5 - 2 \times 10^{-4}$ T and $\Delta B_{pp}^h = 2 - 4 \times 10^{-4}$ T for both the low-field (l) and the high-field (h) components, respectively. In polycrystalline spectra these values increase about 1.7 times: $\Delta B_{pp}^l = 2.5 - 4 \times 10^{-4}$ T and $\Delta B_{pp}^h = 4 - 6 \times 10^{-4}$ T. The ratios of line widths $\Delta B_{pp}^h / \Delta B_{pp}^l \approx 1.5$ and relative intensities $I_{\text{rel}}^h / I_{\text{rel}}^l \approx 1.5$ are the same in spectra of single crystals and of polycrystalline samples.

Eigenvalues of diagonalized g and T tensors of the CH_3 radical in microcline and hyalophane and their direction cosines are listed in Table 3. A comparison with the data of Matyash et al. (1981, 1982) is possible because they measured the central quartet, i.e., the 1:3:3:1 quartet of CH_3 . However, they interpreted this quartet as one of the three quartets of NH_4^+ with magnetic quantum number $m_N = 1, 0, -1$ (see below).

Irradiation causes a significant increase of the relative intensity I_{rel} of the methyl spectrum in microcline. After irradiation with 1×10^6 Gray, I_{rel} increased about 7.5 times, and saturation of the center concentration is at-

TABLE 3. Eigenvalues and direction cosines* of diagonalized **g** and **T** (MHz) tensors of CH₃ in microcline and hyalophane

Feldspar	Eigenvalues	Direction cosines			References
		X	Y	Z	
Microcline, hyalophane	$g_{xx} = 2.0089$	0.95	0.04	-0.30	this work
	$g_{yy} = 1.9992$	0.05	0.99	0.00	
	$g_{zz} = 2.0047$	0.30	0.01	0.95	
	$T_{xx} = 5.8$	0.55	0.67	0.50	
	$T_{yy} = -9.0$	-0.82	0.36	0.44	
	$T_{zz} = 3.1$	0.11	-0.65	0.75	
Microcline**	$A_{\text{iso}} = -71$				Matyash et al. (1981, 1982)
	$T_{xx} = 6.1$	0.55	0.69	0.47	
	$T_{yy} = -9.3$	-0.83	0.40	0.38	
	$T_{zz} = 3.3$	0.07	-0.56	0.78	
	$A_{\text{iso}} = -69$				

* **X** || **a**; **Y** || **b*** or **b**, respectively; **Z** ⊥ **a**, ||(010).

** T_{iso} values were calculated using the A_{xx} , A_{yy} , and A_{zz} values from the original works.

tained. Systematic heating experiments of single crystals show that this center is stable up to about 530 K. The signals disappear reversibly after heating to $T_A = 573$ K (Fig. 6); in the spectrum only the NO₂ triplet remains (cf. below). The same behavior is shown in the methyl spectrum of irradiated hyalophane.

C₂H₅ center. Q band spectra of irradiated hyalophane (Fig. 5, spectrum c) and untreated microcline single crystals (Fig. 7) are better resolved, and additional weak lines can be detected. A careful inspection of this subspectrum gives A values and intensity ratios of the HF components that are typical for the ethyl radical. This spectrum is similar to the 12-line spectrum of ethyl radicals, with nonequivalent α and β protons trapped in γ -irradiated

silica gel and silica glass, giving an intensity ratio of 1:2:3:1:6:3:3:6:1:3:2:1 (cf. Eq. 6 and Fig. 2) and HF constants of $A_{\text{iso}}^{\alpha} = -58.8$ MHz and $A_{\text{iso}}^{\beta} = 73.4$ MHz (Joppien and Willard, 1972). For certain orientations, the spectrum with $N_{\text{HFS}} = 12$ is changed into a spectrum with $N_{\text{HFS}} = 6$. Its intensity ratio is close to the binomial ratio 1:5:10:10:5:1, indicating equal coupling of the unpaired electron with the five protons (Fig. 5, spectrum b). This effect appears in both minerals.

The ratio of relative line intensities I_{rel} of methyl and ethyl spectra is found to be $I_{\text{rel}}^{\text{C}_2\text{H}_5} : I_{\text{rel}}^{\text{CH}_3} \approx 0.25$ in both minerals. Superposition of both spectra leads to a relatively complex HFS pattern (Figs. 5, spectrum c, and 7) with an intensity ratio of 1:6:3:1:18:3:3:18:1:3:6:1, schematically shown in Figure 2.

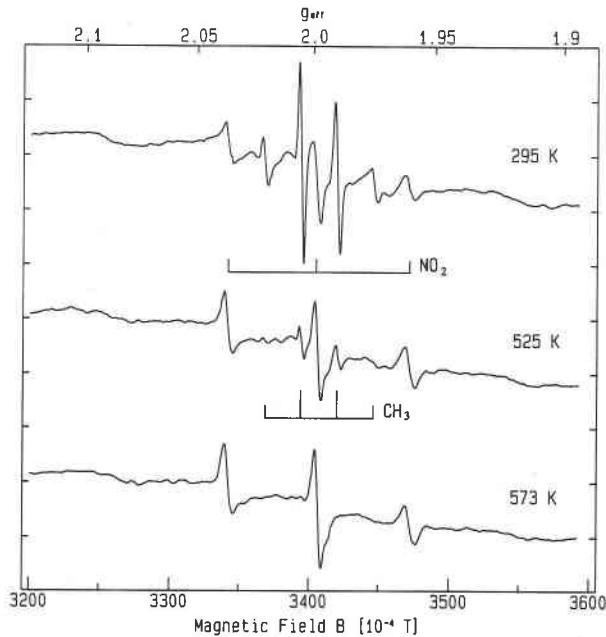


Fig. 6. EPR spectra of microcline heat treated at various annealing temperatures T_A at constant annealing times $t_A = 20$ min. Rotation $+b^* || +Z^0$, $+a || +X^0$, $\theta = 167^\circ$, $m = 9.5239$ GHz, $T = 295$ K.

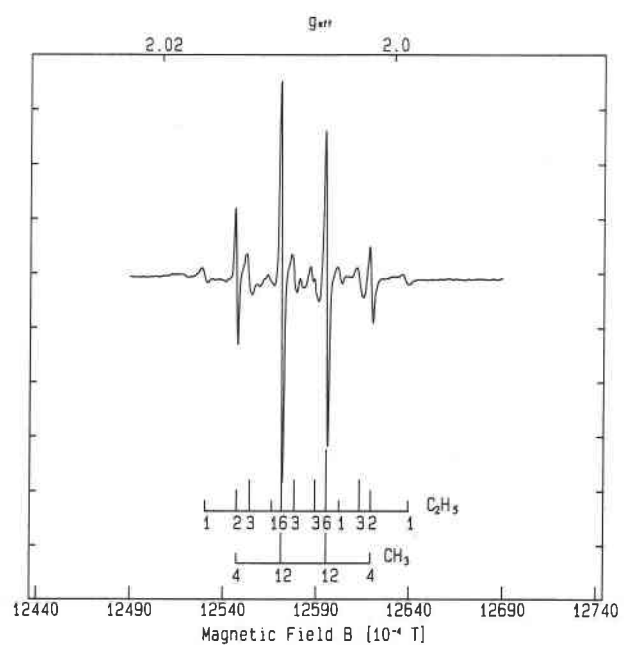


Fig. 7. EPR spectrum of natural microcline. The superposition of the CH₃ and C₂H₅ spectra is schematically marked (cf. Fig. 2). Experimental conditions as in Fig. 5, spectrum c.

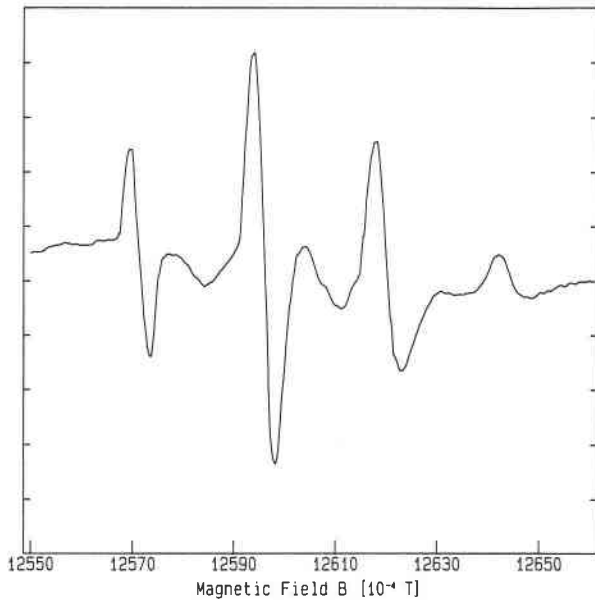


Fig. 8. EPR spectrum of polycrystalline sample of microcline. The random orientation of T with respect to B caused an extreme anisotropic broadening of the CH_2 signals and in the ethyl spectrum could be observed only in the central CH_3 quartet.

Analogous to CH_3 centers, C_2H_5 centers in microcline and hyalophane have the same values of A_{iso} and ΔB_{pp} . For different crystal orientations with respect to B , ΔB_{pp} shows small anisotropy and varies between 4 and 6×10^{-4} T. In polycrystalline spectra the lines of α protons were averaged by anisotropic effects, and only the quartet with the intensity ratio of approximately 1:3:3:1 can be observed (Fig. 8). The behavior of C_2H_5 centers after heat treatment and irradiation is the same as that described for CH_3 centers.

Exact determination of g and T tensors of the ethyl radical and their direction cosines was not possible because of overlapping of the CH_3 , C_2H_5 , and NO_2 room-temperature spectra in both minerals. Low-temperature measurements between 5 and 250 K led to additional overlapping with the 11-line spectra of a'_1 and d_0 -type $O^{1-}/2^{27}Al$ centers, complicating the interpretation further.

The 12-line spectrum observed in microcline, interpreted as NH_3^+ by Matyash et al. (1981, 1982), shows the same behavior after heat treatment and irradiation as the spectra of hydrocarbons in this paper.

Inorganic radicals

$O^{1-}/2^{27}Al$ center. The typical 11-line HFS spectrum of distinct $O^{1-}/2^{27}Al$ centers is present in nearly all irradiated ordered and disordered feldspars. This spectrum can be observed mainly between 5 and 220 K. The temperature of maximum intensity was $T_m \approx 60$ K in all feldspars studied (cf. Table 1). However, in Fe-rich orthoclase from Madagascar and adularia from Hybin pegmatite

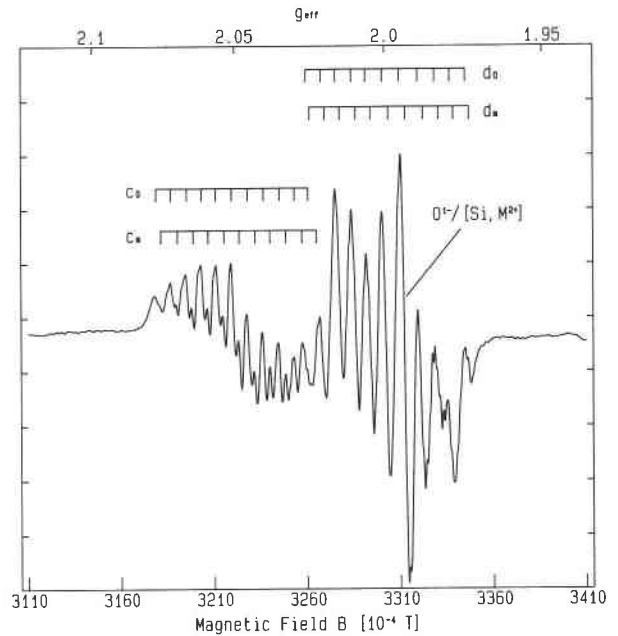


Fig. 9. HFS spectra of the four distinct $O^{1-}/2^{27}Al$ centers, c_0 , c_m , d_0 , and d_m (cf. Fig. 1) in γ -irradiated Amelia albite. The $O^{1-}/2^{27}Al \times 2^{23}Na$ center; a'_1 is superposed by the spectra of d_0 and d_m centers. Rotation $+a \parallel +Z^0$, $+c^* \parallel +X^0$, $\theta = 102^\circ$, $m = 9.2424$ GHz, $T = 60$ K.

with Fe_2O_3 contents of 1–3 wt% (FeO up to 0.25 wt%), no $O^{1-}/2^{27}Al$ centers (or only a very small concentration) and no smoky color was formed after irradiation.

Natural and irradiated alkali feldspars show two main types of $O^{1-}/2^{27}Al$ EPR spectra: (1) spectra of a'_1 , c_0 , d_0 , c_m , and d_m , and d_m centers with an intensity ratio 2:2:2:1:1, and (2) spectra of a'_1 and d_0 centers with an intensity ratio of 3:1. Until now spectra of type 1 have been detected only in well-ordered albite. Spectra of type 2 are observable in ordered and disordered feldspar with large M cations.

In low Amelia albite, spectra of type 1 consist of four sets of superposed 11 HFS patterns because of the distinct $O^{1-}/2^{27}Al$ centers (Fig. 9), discussed in detail by Petrov et al. (1989b). In all feldspars with large M cations ($M = K, Ba$), independent of the degree of Al-Si order, only spectra of 14–15 lines can be observed in certain directions (Fig. 10), created by superposition of the 11-line HFS spectra of two $O^{1-}/2^{27}Al$ centers at distinct O positions. The eigenvalues and eigenvectors of the diagonalized g tensor of the centers in microcline, sanidine, and hyalophane are listed in Table 4. Comparison of the direction cosines of the eigenvectors g_{zz} of the g tensor and T-T directions in the feldspar structure yields an assignment of the centers to O at the Al and D0 position, i.e., a'_1 and d_0 centers (cf. Fig. 1). Their spectra exhibit an intensity ratio $a'_1:d_0$ of about 3:1. The a'_1 centers with the same or similar Hamiltonian parameters were detected in various feldspars by Speit and Lehmann (1982) but were described as b_0 . Their criteria for assigning the cen-

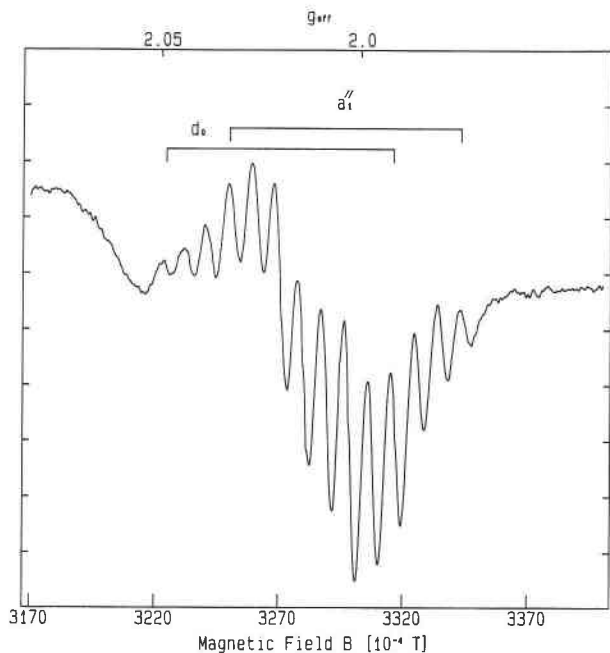


Fig. 10. Typical EPR spectrum of the $O^{1-}/^{227}Al$ centers a_1' and d_0 in γ irradiated ordered and disordered feldspars with large M cations ($M = K, Ba$), e.g., microcline, sanidine, and hyalophane. Rotation $+c^* \parallel +Z^0$, $+a \parallel +X^0$, $\theta = 45^\circ$, $m = 9.2457$ GHz, $T = 60$ K.

ters are based only on considerations of the energetic stabilization of the hole center at an O position with the largest T-O bond. Comparison of the direction cosines of g_{zz} of b_0 centers in Speit (1980) and T-T directions in the

TABLE 4. Eigenvalues and direction cosines* of the diagonalized g tensor of a_1' and d_0 centers at 60 K

Feldspar	PC	Eigenvalues	Direction cosines		
			X	Y	Z
Microcline	a_1'	$g_{xx} = 2.0034$	-0.74	-0.20	0.64
		$g_{yy} = 2.0081$	0.45	-0.86	0.25
		$g_{zz} = 2.0259$	0.49	0.47	0.73
Sanidine	a_1'	$g_{xx} = 1.9997$	-0.77	-0.38	0.50
		$g_{yy} = 2.0069$	0.55	-0.79	0.25
		$g_{zz} = 2.0151$	0.31	0.47	0.83
	d_0	$g_{xx} = 1.9994$	-0.70	-0.54	0.47
		$g_{yy} = 2.0063$	0.67	-0.71	0.19
		$g_{zz} = 2.0257$	0.23	0.45	0.86
Hyalophane	a_1'	$g_{xx} = 1.9954$	0.64	-0.70	0.31
		$g_{yy} = 2.0091$	-0.73	-0.41	0.55
		$g_{zz} = 2.0247$	0.26	0.58	0.77
	d_0	$g_{xx} = 1.9875$	0.73	-0.67	0.15
		$g_{yy} = 2.0232$	-0.60	-0.52	0.61
		$g_{zz} = 2.0245$	0.33	0.53	0.78

Note: PC = paramagnetic center.
* See Table 3.

feldspar structure show that these centers are also a_1' centers. Stereographic projections of the eigenvectors of a_1' and d_0 centers in microcline, sanidine, and hyalophane are given in Figure 11.

The HF tensor A of the $O^{1-}/^{227}Al$ center exhibits a small anisotropy. Its average value is $A_{iso} = 25$ MHz, corresponding to an s-electron density of $c_s^2 = 0.006$ at the ^{27}Al position, and is about the same in all feldspars studied (Speit and Lehmann, 1982; Petrov et al., 1989b). Comparison of the mean values of A_{iso} of centers in quartz and feldspar reveals an increase of covalent character in the Al-O bond of >50% from oxide to the aluminosili-

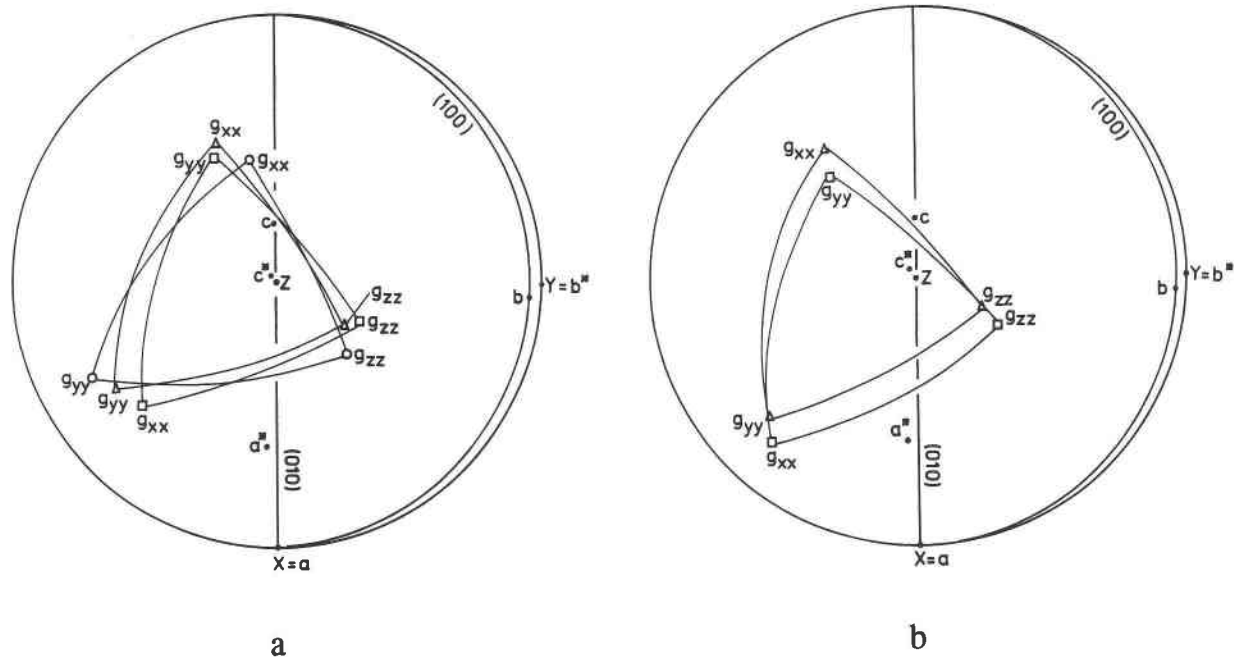


Fig. 11. Stereographic projection of the g eigenvectors from Table 4 of (a) a_1' centers in sanidine (triangles), microcline (circles), and hyalophane (squares) and (b) of d_0 centers in sanidine (triangles) and hyalophane (squares).

TABLE 5. Eigenvalues and direction cosines* of the diagonalized g tensor of $O^{1-}/(Si, M^{2+})$ centers in various feldspars

Feldspar	PC	Eigenvalues	Direction cosines			References
			X	Y	Z	
Labradorite, oligoclase	h(b _m)	$g_{xx} = 1.9917$	-0.35	-0.48	0.80	Speit and Lehmann (1982)
		$g_{yy} = 2.0101$	-0.17	0.88	0.45	
		$g_{zz} = 2.0193$	0.92	0.02	0.39	
Amazonite	h(b _m)	$g_{xx} = 2.0040$	-0.30	-0.64	0.71	this work
		$g_{yy} = 2.0098$	-0.61	0.70	0.37	
		$g_{zz} = 2.0123$	0.73	0.32	0.60	
Hyalophane	h(b)	$g_{xx} = 2.0032$	-0.43	0.50	0.75	this work
		$g_{yy} = 2.0103$	0.10	-0.80	0.59	
		$g_{zz} = 2.0140$	0.89	0.33	0.30	
Microcline	h(c _m)	$g_{xx} = 2.004$	0.99	-0.08	0.07	Matyash et al. (1981, 1982); this work
		$g_{yy} = 2.010$	-0.05	-0.20	0.98	
		$g_{zz} = 2.056$	0.09	0.98	0.19	
Albite	h(c _m)	$g_{xx} = 2.0077$	-0.89	-0.43	0.13	Petrov et al. (1989b)
		$g_{yy} = 2.0228$	0.45	-0.84	0.31	
		$g_{zz} = 2.0618$	0.02	0.34	0.94	

Note: PC = paramagnetic center.

* See Table 3.

cate. The widths of the individual lines are $\Delta B_{pp} = 4 \pm 0.5 \times 10^{-4}$ T; ΔB_{pp} , as well as A_{iso} , did not change between 5 and 220 K. This indicates that the lifetime of the excited states does not influence ΔB_{pp} . The large line widths observed in all feldspars compared with those of Al centers in, e.g., smoky quartz (e.g., Mackey, 1963; Schnadt and Schneider, 1970) must be due to other phenomena, most probably to unresolved HF interactions with nuclear magnetic moments of adjacent atoms (e.g., Na, Al) or to some disorder in the Al-Si occupancy of adjacent tetrahedra.

$O^{1-}/(Si, M^{2+})$ center. In addition to the $O^{1-}/2^{27}Al$ centers distinct $O^{1-}/(Si, M^{2+})$ centers were found in all investigated crystals of ordered and disordered feldspars. The spectrum of these centers consists of one single line ($\Delta B_{pp} = 6 \pm 0.5 \times 10^{-4}$ T) and can be observed between 5 and 295 K with $T_m \approx 5$ or 115 K for different feldspars. No HFS could be detected in this temperature range. The angular dependence of the spectrum on crystal rotation with respect to \mathbf{B} is described by the first term, $\beta \mathbf{B} \mathbf{g} \mathbf{S}$, of Equation 2.

Centers of this type were described as existing in irradiated microcline, labradorite, oligoclase, and albite (Marfunin and Berskov, 1970; Speit and Lehmann, 1982; Petrov et al., 1989b). Eigenvalues and direction cosines of the diagonalized g tensor of this center in different feldspars with respect to T-O directions in the feldspar structure are presented in Table 5. The data from the center in microcline from the Hagendorf pegmatite are approximately the same as those of microcline from granites and pegmatites of the Ukrainian Shield (Matyash et al., 1981, 1982). The stereographic projections of the eigenvalues of the g tensor of this center for various feldspars are plotted in Figure 12.

NO_2 center. As shown in Figure 6, in the spectrum of microcline the methyl and ethyl signals disappear after heating at $T_A = 573$ K. In heat-treated microcline and untreated hyalophane (Figs. 4 and 5, spectrum a), the typical spectrum of NO_2 could be observed. The NO_2

center can be identified by its characteristic HFS spectrum of three equidistant lines of equal intensity. A HFS pattern of this type is due to the interaction of an unpaired electron ($S = 1/2$) with a N nucleus ($I = 1$, 99.63% natural abundance of ^{14}N). Analogous to hydrocarbon centers, NO_2 centers in microcline and hyalophane have the same values of A_{iso} and ΔB_{pp} . For different crystal orientations with respect to \mathbf{B} , ΔB_{pp} is anisotropic and varies between 5 and 10×10^{-4} T.

A spectrum of this type was observed first in microcline

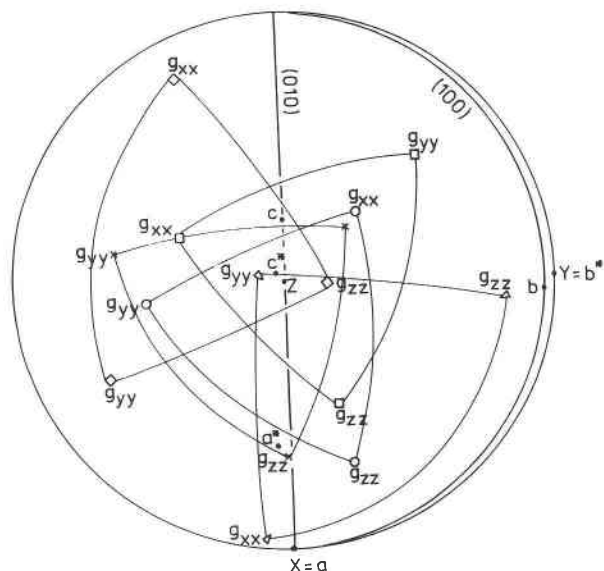


Fig. 12. Stereographic projection of the g eigenvectors of $h(b_m)$, $h(c_m)$, and $h(d_m)$ centers from Table 5 in various feldspars; squares = amazonite, triangles = microcline, diamonds = albite, \times = labradorite, circles = hyalophane. The g_{zz} eigenvector of the $h(c_m)$ center in microcline lies about 10° from the b^* axis, and those of the $h(d_m)$ center in albite about 20° from the c^* axis. The centers in amazonite, labradorite, and hyalophane are $h(b_m)$ centers.

TABLE 6. Hamiltonian parameters of N-associated paramagnetic centers in various matrices

Host crystal	PC	T (K)	g tensor			T tensor* (MHz)			A_{iso}	References
			g_{xx}	g_{yy}	g_{zz}	T_{xx}	T_{yy}	T_{zz}		
Diamond	N		2.0035	2.0025	2.0014	-1.7	-1.7	3.4	16.5	Poole et al. (1977)
Diamond	N		2.0020	2.0020	2.0020	-10.2	-10.2	20.4	86.1	Poole et al. (1977)
Diamond	C-N-N-C		2.0030	2.0030	2.0030	-12.6	-12.6	25.2	96.3	Poole et al. (1977)
Diamond	N-C-N		2.0028	2.0028	2.0028	-11.3	-11.3	22.6	93.0	Poole et al. (1977)
KN ₃	N ₂ **	77	2.0027	2.0008	1.9832	-14.6	-15.1	29.7	3.92	Atkins and Symons (1967)
Beryl	NO ₂	77	2.0213	2.0213	2.0023	-1.0	-1.0	1.9	11.3	Solntzev (1981)
Pb(NO ₃) ₂	NO ₂	77	2.029	2.029	1.998	-2.0	-2.0	3.6	4.8	Ayscough (1967)
KNO ₃	NO ₂ ⁻	77	2.008	2.010	2.007	-26.6	-26.6	53.2	36.4	Ayscough (1967)
KCl	NO ₂ ⁻	223	2.0070	2.0099	2.0069	-20.4	-26.0	46.5	40.0	Ayscough (1967)
KCl	NO ₂ ⁻	83	2.0068	2.0068	2.0020	-28.8	-28.8	58.0	114.2	Ayscough (1967)
Ice	NO ₂	77	2.0066	1.9920	2.0022	-17.6	-19.6	37.2	159.3	Ayscough (1967)
KCl	NO ₂	—	2.0003	2.0003	2.0014	-17.9	-17.9	36.1	157.1	Ayscough (1967)
NaNO ₂	NO ₂	—	2.0057	1.9910	2.0015	-14.8	-22.1	36.9	153.2	Ayscough (1967)
KNO ₃	NO ₂	—	2.0036	1.9910	2.0036	-11.1	-11.1	22.3	153.1	Wertz and Bolton (1972)
AgNO ₃	NO ₂	77	2.0090	1.9978	2.0039	-15.7	-21.8	37.2	157.6	Pietrzak and Wood (1970)
NaX zeolite	NO ₂	77	2.0043	1.9922	2.0015	-13.4	-18.8	32.5	156.5	Pietrzak and Wood (1970)
CaX zeolite	NO ₂	77	2.0051	1.9921	2.0017	-10.9	-22.4	33.0	156.2	Pietrzak and Wood (1970)
Beryl	NO ₂	77	2.0064	1.9925	2.0020	-12.6	-18.8	31.4	152.6	Suharzhovskyi (1976), Solntzev (1981)
Microcline†	NO ₂	77	2.006	1.992	2.006	-6.7	-21.8	28.6	164.6	Matyash et al. (1981, 1982)
Microcline	NO ₂	77	2.0041	1.9913	2.0031	-6.8	-22.8	29.6	167.0	this work
Hyalophane	NO ₂	30	2.0048	1.9910	2.0011	-7.7	-21.9	29.8	170.7	this work

Note: PC = paramagnetic center.

* See Table 3.

** Cited as N²⁻ in Matyash et al. (1981).

† Interpreted as N²⁻.

from Ukrainian Shield granites and pegmatites by Matyash et al. (1981, 1982) and interpreted as N²⁻. Comparison of the EPR data of Matyash et al. (1981, 1982) and Hamiltonian parameters of N-associated paramagnetic centers in different host crystals (Table 6) shows evidently that their center is also NO₂. The direction cosines of the diagonalized **g** and **T** tensors of the NO₂ radical in hyalophane and microcline from Hagendorf pegmatite (Table 7) are in good agreement with the data of Matyash et al. (1981, 1982).

The calculated values of c_s^2 , c_{pz}^2 , and ρ from Equations 4, 5, 7, and 8 for NO₂ in hyalophane and microcline at various temperatures are given in Table 8. These values are typical for triatomic radicals with 17 valence electrons (Atkins and Symons, 1967; Carrington and McLachlan, 1967) and may be compared with the data for NO₂ in beryl (Suharzhovskyi, 1976; Solntzev, 1981). The O-N-O angles ρ estimated on the basis of Equation 8 for various temperatures are between 129–138 and 130–140° for hyalophane and microcline, respectively (Table 8).

TABLE 7. Eigenvalues and direction cosines* of the diagonalized **g** and **T** (MHz) tensors of NO₂ with $\rho = 138^\circ$ in microcline and hyalophane at different temperatures

Feldspar	T (K)	Eigenvalues	Direction cosines			References
			X	Y	Z	
Microcline*	77	$g_{xx} = 2.006$	0.27	0.96	0.02	Matyash et al. (1981, 1982)
		$g_{yy} = 1.992$	0.02	-0.01	0.99	
		$g_{zz} = 2.006$	0.96	0.27	-0.02	
		$T_{xx} = -6.7$	-0.47	0.85	0.22	
		$T_{yy} = -21.8$	0.09	-0.20	0.98	
		$T_{zz} = 28.6$	0.87	0.49	0.02	
Microcline	77	$g_{xx} = 2.0041$	0.32	0.94	-0.11	this work
		$g_{yy} = 1.9913$	0.00	0.12	0.99	
		$g_{zz} = 2.0031$	-0.95	0.32	-0.04	
		$T_{xx} = -6.8$	0.43	0.89	-0.13	
		$T_{yy} = -22.8$	0.18	0.06	0.98	
		$T_{zz} = 29.6$	0.88	-0.44	-0.13	
Hyalophane	30	$g_{xx} = 2.0048$	0.38	-0.92	0.00	this work
		$g_{yy} = 1.9910$	0.00	0.00	1.00	
		$g_{zz} = 2.0011$	0.92	0.38	0.00	
		$T_{xx} = -7.7$	0.02	0.97	0.21	
		$T_{yy} = -21.9$	0.08	0.21	0.97	
		$T_{zz} = 29.8$	0.99	0.00	0.08	

* See Table 3.

TABLE 8. Calculated unpaired electron-spin density coefficients c_s^2 , c_{pz}^2 , and c_o^2 and O-N-O bond angles ρ of the NO_2 radical in hyalophane, microcline, and beryl at various temperatures

Host crystal	T (K)	c_s^2	c_{pz}^2	c_o^2	λ^2	ρ (°)	References
Hyalophane	295	0.094	0.322	0.584	3.430	129	this work
	150	0.095	0.349	0.556	3.678	130	
	77	0.096	0.403	0.501	4.203	133	
	50	0.095	0.472	0.433	4.967	136	
	30	0.094	0.537	0.369	5.710	138	
Microcline	295	0.092	0.328	0.580	3.565	130	this work
	150	0.093	0.334	0.573	3.572	130	
	77	0.092	0.532	0.376	5.770	138	
	50	0.093	0.598	0.309	6.430	140	
	30	0.093	0.610	0.297	6.559	140	
Microcline*	295	0.090	0.320	0.590	3.562	130	Matyash et al. (1981, 1982)
	77	0.091	0.515	0.394	5.661	138	
Beryl*	77	0.084	0.565	0.351	6.726	140	Suharzhovsky (1976), Solntzev (1981)

* The c_s^2 , c_{pz}^2 , c_o^2 , and ρ values from Eqs. 4, 5, 7, and 8 were calculated using the original data and the corrected $^{14}\text{A}_{\text{iso}}^*$ and $^{14}\text{T}^*$ for the free N atom after Morton and Preston (1978).

The NO_2 center is observable in natural single crystals and polycrystalline samples. Irradiation with a γ dose up to about 2×10^6 Gray causes the spectrum intensity to decrease by a factor of 16 (cf. spectra a and b in Fig. 5). The annihilation temperature of the center is $T_A \approx 873$ K. After being heated above this temperature, the center is destroyed irreversibly. Heat treatment at about 823 K causes an increasing of the signal intensity of about 50% (Fig. 13). The same behavior showed the center described by Matyash et al. (1981).

SiO_3^- center. An electron captured at an O vacancy of the SiO_4 tetrahedron forms the 25-electron radical SiO_3^- . A center of this type with additional HFS from one adjacent ^{27}Al nuclei was detected in microcline by Matyash et al. (1981, 1982). The center was attributed to an electron captured at a vacancy on the B0 O position, forming an $e(b_o)$ center. The same center, but without HFS from a neighboring ^{27}Al nucleus, can also be detected in the spectra of most feldspars studied, but, because of the absence of HFI with ^{27}Al , this center must be attributed to an O vacancy at an O_m position (e_m center) in the feldspar structure. The approximately isotropic g allows no unambiguous assignment of this center to specific O vacancies.

DISCUSSION

Hydrocarbon radicals

The typical 12-line spectrum of ethyl radicals with the intensity ratio of 1:2:3:1:6:3:3:6:1:3:2:1 was observed in microcline first by Matyash et al. (1981, 1982), though it was assigned to NH_3^+ radicals at M positions (Fig. 14b). However, it is generally assumed that, because of the rotation of the NH_3^+ radical, the three protons are equivalent. In this case, the HF interaction between S and I leads to multiple sets of $(2I_N + 1)(2nI_H + 1)$ lines. Because $I_N = 1$, $I_H = 1/2$, and $n = 3$, the NH_3^+ spectrum consists of three quartets (1:3:3:1) of equal intensities, corresponding to the three allowed orientations of the ^{14}N nuclear spin (magnetic quantum number $m_N = +1, 0,$

–1) with respect to **B**. The typical NH_3^+ spectrum with an intensity ratio of 1:1:3:1:3:3:3:1:3:1:1 is caused by the disposition of the three quartets. Such a spectrum, caused by NH_3^+ trapped in a single crystal of NH_4ClO_4 , is shown in Figure 14a. The same spectrum was reported for NH_3^+ in structural channels of beryl (Solntzev, 1981). However, these centers are thermally much more stable than those reported by Matyash et al. (1981, 1982); their annihilation temperature is 1.6 times higher. After heat treatment at 773 K, NH_3^+ decays into $\text{NH}_2 + \text{H}^+$, and the characteristic spectrum of NH_2 can be observed. This

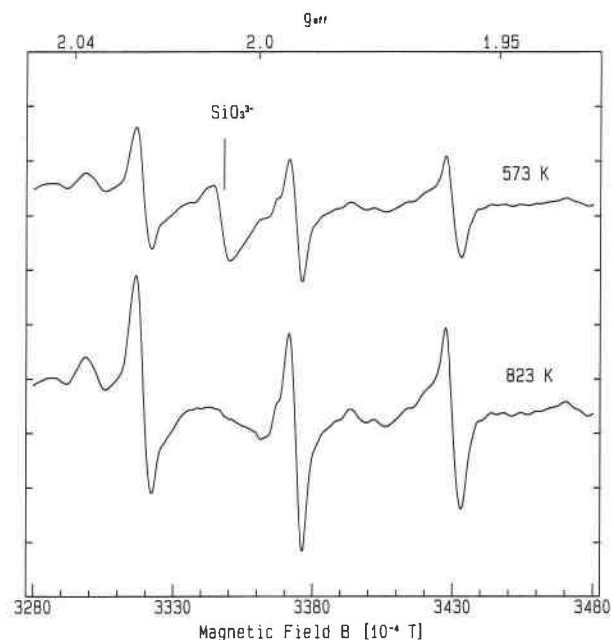


Fig. 13. EPR spectra of microcline after bleaching the spectra of hydrocarbons at annihilation temperature $T_A = 573$ K. After further heating at $T_A = 823$ K, the signal intensity increased about 50%. In both experiments $t_A = 20$ min. Experimental conditions as in Fig. 6.

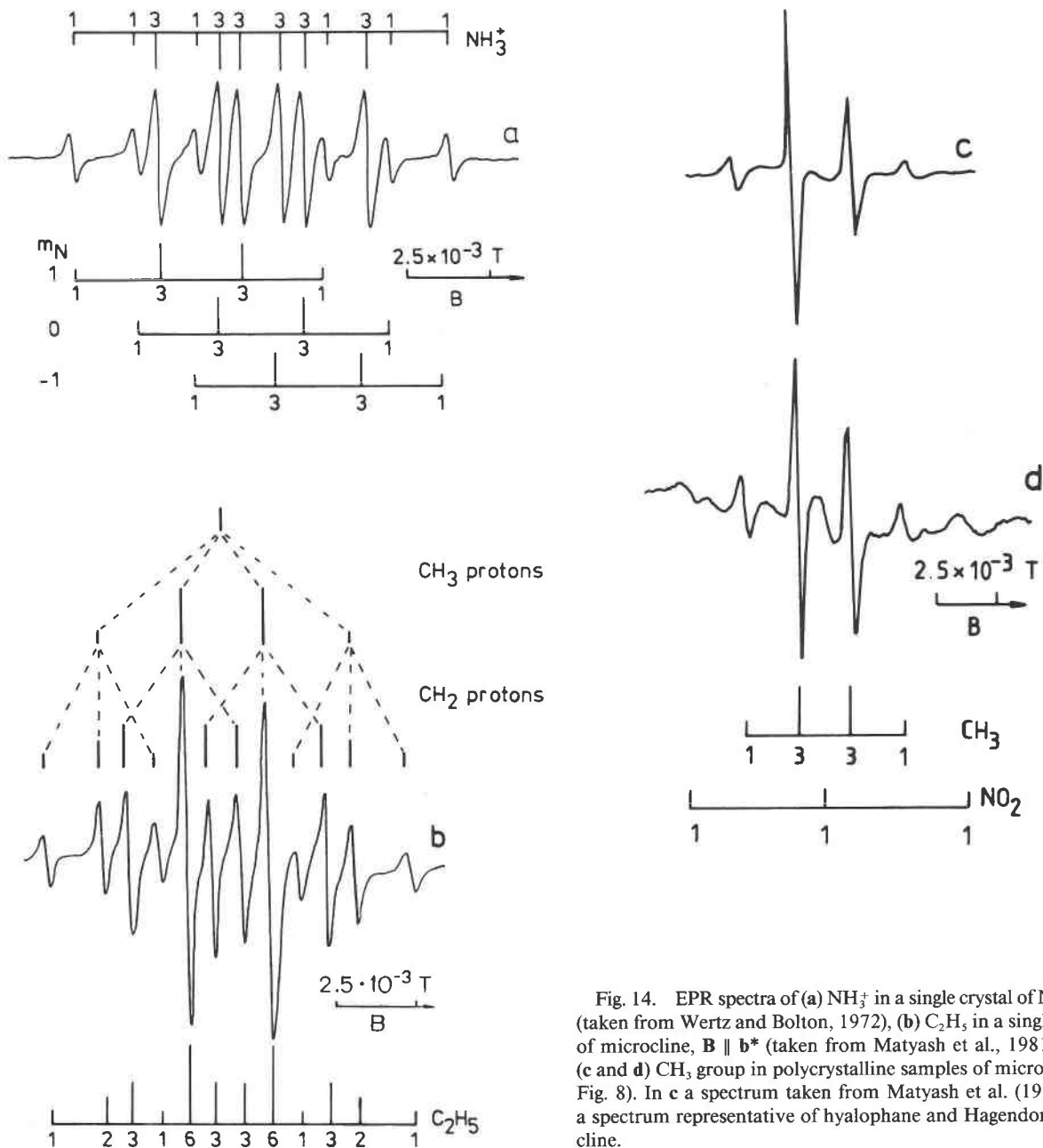


Fig. 14. EPR spectra of (a) NH_3^+ in a single crystal of NH_4ClO_4 (taken from Wertz and Bolton, 1972), (b) C_2H_5 in a single crystal of microcline, $\mathbf{B} \parallel \mathbf{b}^*$ (taken from Matyash et al., 1981, 1982), (c and d) CH_3 group in polycrystalline samples of microcline (cf. Fig. 8). In c a spectrum taken from Matyash et al. (1981), in d a spectrum representative of hyalophane and Hagendorf microcline.

feature cannot be seen in spectra of microcline. The behavior after heat treatment and irradiation of the centers described by Matyash et al. (1981, 1982) is exactly the same as those of the hydrocarbon centers reported in this paper.

A careful inspection of the spectrum of Matyash et al. (1981 and 1982, their Figs. 46 and 1, respectively) shows an intensity ratio of the lines that is typical for the ethyl radical (cf. Figs. 2 and 14b). The ratio $A_{\text{iso}}^\alpha/A_{\text{iso}}^\beta = 0.8$ of α and β protons of the ethyl radical is in good agreement with the results of this paper and with theoretical and

experimental data (Jen et al., 1958; Fessenden and Schuler, 1963; Bersohn and Baird, 1966; Ayscough, 1967; Carrington and McLachlan, 1967; Wertz and Bolton, 1972).

For free radicals in fluids of low viscosity, the molecular tumbling rate is sufficiently rapid that the anisotropic g and T are averaged to zero. Line widths of $\Delta B_{pp} \approx 0.1 \times 10^{-4}$ T or less are common (e.g., Ayscough, 1967). In fluids of moderate viscosity, the tumbling rate decreases, and ΔB_{pp} increases ($\approx 0.3 \times 10^{-4}$ T) (e.g., Fessenden and Schuler, 1963). For radicals trapped in single crystals the

tumbling rate decreases further, and deviation of Δg_{ii} and T_{ii} from zero is evident, accordingly the value of ΔB_{pp} increases. However, ΔB_{pp} is proportional to the mean square of the shift in line positions and is different for each line. If A_{iso} is positive, the high-field HF components are broader, i.e., the derivate amplitude is lower (Wertz and Bolton, 1972). In spectra of randomly oriented polycrystalline matrices these effects are more pronounced.

In the hydrocarbon spectra of single crystals of microcline and hyalophane the influence of these effects is evident. In comparison with the values expected for hydrocarbon radicals in fluids, ΔB_{pp}^{β} of low- and high-field components of the central quartet are up to 20 and up to 40 times broader, respectively. Asymmetry in line shape and width and therefore in the line intensities of the quartet is caused by the superposition of the spectra of α protons of the methyl radical and β protons of the ethyl radical. Because the rotation of β protons is fixed in a plane perpendicular to the C-C axis, their rotation in the larger ethyl radical, trapped in a single crystal, is more constrained than the relatively freely rotating α protons of the methyl radical. Therefore the HFI of the α protons of the methyl radical has a smaller anisotropy, each quartet is nearly symmetric, and the values of ΔB_{pp}^{α} are smaller. On the other hand, the anisotropy of HFI of the β protons of the ethyl radical is larger, and the values of Δ_{pp}^{β} increase and are different for each component. This causes the asymmetry in line shape and intensity of the central quartet in the superposed spectra of methyl and ethyl radicals. Because of the positive sign of A_{iso}^{β} , the high-field components have larger ΔB_{pp}^{β} and lower J_{rel}^{β} values than those of the low-field components of the quartet. By overlapping of methyl and ethyl spectra in microcline and hyalophane, the anisotropic effects dominate and explain the asymmetry of the spectra. In polycrystalline spectra these effects are evident. The approximately equal A_{iso} and T_{ii} values of the α protons in the $-\text{CH}_2$ group lead to additional line broadening (up to 60 times broader than in fluids) in the single-crystal spectra of both minerals. Consequently, in their polycrystalline spectra the random orientation of **T** with respect to **B** causes an extreme line broadening; no lines of the ethylene group could be detected. Only the superposition of the spectra of the α and β protons of the methyl and ethyl radicals, respectively, could be observed (Fig. 8).

The organic free radicals, by virtue of their great reactivity, are not stable in fluids (inclusions) and are not stabilized by surfaces of solid substrates at room temperature. In almost all cases, spectra of these radicals can be detected only after continued ionizing irradiation at low temperatures (<200 K). The average lifetime of methyl and ethyl radicals in fluids at temperatures <200 K is about 10^{-3} s (Fessenden and Schuler, 1963; Bljumenfeld et al., 1966; Ayscough, 1967; Wertz and Bolton, 1972). The lifetime of methyl and ethyl radicals adsorbed in silica gel during γ irradiation at 77 K is a few minutes after reaching ≤ 260 K (Bljumenfeld et al., 1966; Joppien and Willard, 1972). After warming from 77 to 129 K,

95% of the CH_3 quartet observed by Joppien and Willard (1972) in silica glass had decayed, and a second spectrum of the more stable species $\text{CH}_2\text{-O-Si}<$ was detected. In addition these species decayed rapidly at room temperature. Lattice-stabilized methyl radicals in quartz, stable at room temperature, reported by Ikeya et al. (1986) and Matyash et al. (1987), show similar annihilation temperatures ($T_A = 573$ K during $t_A = 15$ min and $T_A = 523$ K during $t_A = 1$ h, respectively) as in feldspar. Structurally bonded CH_3 radicals in enstatite, beryl (Bershov, 1970; Edgar and Vance, 1977), and zeolite (Noble et al., 1967) have T_A between 573 and 773 K.

The behavior of the methyl and ethyl spectra in microcline and hyalophane after heat treatments and irradiation indicated that these radicals are formed from methane and ethane by the production of H after natural or artificial irradiation. The diffusion of protons from CH_4 radicals to a nearby Fe^{3+}O_4 tetrahedral complex, creating thermally stable ($T_A > 1273$ K, $t_A > 113$ h) $\text{Fe}^{3+}\text{O}_2(\text{OH})_2$ centers, is demonstrated by the EPR spectra of irradiated hydrocarbon-bearing hyalophane crystals (Petrov, 1992). The anisotropic nature of the spectra and the high annihilation temperature ($T_A = 573$ K) of the methyl and ethyl radicals suggest that the hydrocarbons are structurally bonded in both feldspars. It is likely that CH_4 resides in the M site of the microcline and hyalophane structure in view of the fact that isoelectronic NH_4^+ occurs in the M site of buddingtonite. The NH_4^+ is irregularly coordinated by nine O atoms, O_A2 at 2.95 Å and eight others at distances ranging from 3.01 to 3.18 Å (Kimball and Megaw, 1972). The C-H and C-C distances in methane and ethane are 1.09 and 1.53 Å, respectively. NH_4^+ substitution for K^+ and Na^+ in synthetic alkali feldspar was experimentally demonstrated by Barker (1964). Substitution is more rapid in alkali feldspars of intermediate composition than in either pure Na or K end-members at a hydrothermal condition of $P = 2$ kbar and $T = 823\text{--}973$ K. It seems apparent that small amounts of methane and ethane can reside in the larger M positions with a slight local expansion of the microcline and hyalophane structures.

With hyalophane samples from the same locality and with the same chemical composition as those used in this study, Beran et al. (1992) determined 0.12 wt% N by microprobe analysis and assigned the vibrational bands in the infrared region at about $2800\text{--}3600$ cm^{-1} to NH_4^+ (which is isoelectronic with CH_4). However, after irradiation of the hyalophane crystals, only EPR spectra of CH_3 and none of NH_3^+ were detected. Using EPR, N-associated centers are detectable only in the form of NO_2 radicals.

O¹⁻ radicals

Generally, the formation of $\text{O}^{1-}/^{227}\text{Al}$ centers in feldspar is dependent on small deviations in thermodynamic conditions during crystallization and postcrystallization processes and the distribution of Al and Si over the four nonequivalent tetrahedral positions T10, T1m, T20, and

T2m. Centers of this type may be formed where two adjacent tetrahedral positions on either side of an O atom are occupied by Al atoms, building an Al-O-Al bridge. The detectable HF interaction of the electronic spins of O^{1-} centers with nuclear magnetic moments of two neighboring ^{27}Al and their assignments to crystallographic positions based on comparison of the direction cosines of the \mathbf{g} tensor and T-T directions (Fig. 1) allow the direct measurement of the Al migration, e.g., the exchange of Al and Si among the tetrahedral sites in order-disorder processes.

The values of line width ΔB_{pp} , HF coupling constant A , and center concentration and therefore T_m of the $O^{1-}/^{27}\text{Al}$ centers are approximately equal in all feldspars studied, independent of their degree of long-range Al-Si order. This indicates a similar degree of Al-Si order around the center; i.e., in all feldspars such centers can be formed only in intracrystalline domains of similar order. If such domains can be considered as frozen states of Al distribution then the position and frequency of different Al- O^{1-} -Al fragments may yield information about short-range Al site occupancy and, therefore, about ordering paths in feldspar. The intensity ratio of the HFS spectra of a'_1 , a''_1 , c_o , d_o , c_m , and d_m centers, i.e., the ratio of their concentrations, allows the direct measurement of Al site occupancies at definite tetrahedral positions. The short-range Al site occupancy in potassium feldspar and barium feldspar in a short EPR length scale (for Al- O^{1-} -Al bridges on the order of 10^{-4} pfu) is approximately equal to $t_{1o} \approx t_{1m} \gg t_{2o} \approx t_{2m}$. Here, t_{1o} , t_{1m} , etc., refer to the site occupancies of Al at positions T10, T1m, etc., respectively. This suggests a short-range ordering path of the intermediate two-step trend (e.g., Ribbe, 1983; Kroll and Ribbe, 1983). In low albite with $t_{1o} \approx t_{2m} > t_{1m} \approx t_{2o}$, the ordering path tends more to the one-step trend. However, to answer this question with certainty, a comparison with other methods is necessary.

The absence (or very low concentration) of $O^{1-}/^{27}\text{Al}$ centers in Fe-rich orthoclase and adularia after long-term irradiation may be explained by a possible compensation of the positive charge deficiency in the Al-O-Al segments that violate the principle of Loewenstein by the substitution of Fe^{2+} for K^{1+} , i.e., $\text{K}^{1+} + \text{Si}^{4+} \rightarrow \text{Fe}^{2+} + \text{Al}^{3+}$, similar to the case of amazonite with high Pb^{2+} content (Petrov et al., 1993). Thus, no stable $O^{1-}/^{27}\text{Al}$ centers and, therefore, no smoky color can be induced by irradiation. In orthoclase and adularia with sluggish Al-Si exchange kinetics and high Fe_2O_3 content, the line intensity of Fe^{3+} at the T1 tetrahedral position is about ten times higher than those of Eifel sanidine with anomalous rapid Al-Si exchange kinetics (Petrov, in preparation). The FeO_4 tetrahedron ($\text{Fe-O} = 1.862 \text{ \AA}$) has a quasi-orthorhombic distortion of 9.3° from cubic symmetry of the two opposite tetrahedral angles O-Fe-O (Petrov and Hafner, 1988). At the boundaries between ordered and disordered domains in the feldspar structure, such an angular distortion of the tetrahedron can have a stabilizing

effect. A similar effect was found for Fe^{3+}O_4 tetrahedra with quasi-orthorhombic distortion embedded in the boundaries between ordered and disordered sections of the SiO_4 matrix in acid volcanic glasses (Bershov et al., 1983).

The Al-Si exchange in feldspar seems to be facilitated by $O^{1-}/^{27}\text{Al}$ centers, OH^- , and H_2O (Beran, 1986; Petrov and Hafner, 1988), whereas Fe^{3+} obviously can have a stabilizing effect. Furthermore, with increasing total Fe_2O_3 content the concentration of $O^{1-}/^{27}\text{Al}$ centers decreases and the Al-Si exchange kinetics becomes more sluggish.

In all investigated natural and irradiated feldspars with different degrees of Al-Si order distinct $O^{1-}/(\text{Si}, \text{M}^{2+})$ centers are present. Since the center is apparently not perturbed by HFI with an adjacent nuclear moment, it is generally assumed that it occurs at O positions that are not bridging to Al tetrahedra. For O^{1-} stabilization at room temperature a charge of $<3+$ at one of the adjacent tetrahedral positions is needed. Divalent ions that possess abundant isotopes without nuclear moments are most likely for M, e.g., Mg^{2+} or a divalent cation with a small radius at a T1m position. The $O^{1-}/(\text{Si}, \text{M}^{2+})$ center without HFS of the adjacent ^{27}Al most probably can be created at D_m , C_m , B_m , or A_2 O positions. In the investigated crystals of feldspar, the g_{zz} eigenvalues of the \mathbf{g} tensor of the 31-electron radical SiO_3^- can be attributed to the T20-Bm, T20-Cm, and T20-Dm directions. The $O^{1-}/(\text{Si}, \text{M}^{2+})$ centers in most feldspars investigated so far with different degrees of Al-Si order are $h(b_m)$, $h(c_m)$, and $h(d_m)$ centers (Table 5). The $h(b_m)$ centers in labradorite and oligoclase were determined as $h(b_o)$ by Speit and Lehmann (1982). In this case, however, HFS due to interaction with at least one adjacent ^{27}Al nuclei at the T10 position should be observable in the spectra (cf. Fig. 1).

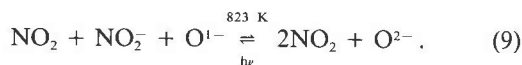
NO_2 radicals

Matyash et al. (1981, 1982) attributed the triplet in the spectrum of heat-treated microcline (Fig. 6) to a N^{2-} center at the D_m O position ($\text{Si-N}^{2-}\text{-Si}$). Matyash et al. (1981, their Table 13) based their interpretation on a comparison with Hamiltonian parameters of N^{2-} centers from Atkins and Symons (1967). However, in the original work N^{2-} centers are not reported; the parameters cited are from N^{2-} pairs. This comparison is retracted by Matyash et al. (1982).

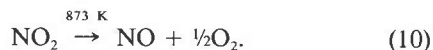
For NO_2 in different host crystals HF constants were measured (Table 6) that correspond to coefficients of c_2^2 between 0.084 and 0.1. The large s-fraction c_2^2 in the wave function of the unpaired N electron and the relatively small 2p/2s ratio λ^2 (Table 8) is characteristic only for the NO_2 radical (Atkins and Symons, 1967; Ayscough, 1967; Wertz and Bolton, 1972). The molecular parameters and O-N-O angles of NO_2 in microcline and hyalophane (Table 8) are in good agreement with published data of NO_2 in many host matrices (e.g., Atkins and Symons, 1967). Contrary to these data, the unpaired elec-

tron of other NO_m^{\cdot} radicals listed in Table 6 is localized in an orbital with a predominant p fraction. For example, values of $c_s^2 = 0.026$, $c_{pz}^2 = 0.54$, and $\lambda^2 = 24$ were calculated for NO_2^- centers in single crystals of NaCl and KNO_3 ; i.e., the unpaired electron is located in a nearly pure p orbital. The remaining 40% of the electron density is delocalized at the O atoms (Atkins and Symons, 1967). For the ^{14}N - ^{13}C bonding in type I diamond, Shcherbakova et al. (1969, 1972) determined values of A_{iso} , corresponding to $c_s^2 = 0.051$. They localized the unpaired electron in an antibonded p orbital. Smith et al. (1959) investigated the same type of diamond and calculated 12.5% s and 87.5% p fraction for the sp^2 hybrid of the ^{14}N - ^{13}C segment.

The behavior of the spectrum after heat treatment and irradiation may be explained by the postulation of a substitution of NO_2 for K^+ . A part of these radicals can trap electrons by natural irradiation and is transformed into the diamagnetic NO_2^- state. These radicals can be regarded as electron centers, complementary to the distinct O^{1-} hole centers (a'_i , d_o , and h_m) in the structure of microcline and hyalophane. Thus, compensation for the energetically unfavorable accumulation of positive charges at the O^{1-} ion is given, and at low temperatures the hole is stabilized at this O atom. In addition, yielding of electrons transforms this part of the radicals into their paramagnetic form NO_2^{\cdot} :



In accordance with this interpretation, heat treatments at $T_A = 823 \text{ K}$ of irradiated crystals caused a decay in the spectra of all types of radiation-induced O^{1-} centers and an increase in the line intensity of the NO_2 spectrum (Fig. 13). According to Equation 9, the remaining 50% of these radicals were transformed by heat treatment at 823 K into their paramagnetic state by recombination of NO_2^- electrons and O^{1-} holes. Irradiation caused a significant decrease in the NO_2 spectrum (cf. Fig. 5, spectra a and b) and the creation of the distinct O^{1-} centers with spectra of high intensity. The same behavior was reported by Matyash et al. (1981) for N^{2-} centers, but omitted in Matyash et al. (1982). After heat treatment at 873 K, all NO_2 centers were destroyed irreversibly. After irradiation up to 2×10^6 Gray, the centers cannot be restored. A possible model for the mechanism of center destruction may be given by



In fluids NO_2 tends to form dimers rapidly, producing diamagnetic N_2O_4 . Isolated NO_2 free radicals can be produced in situ only by ionizing irradiation at low temperatures (4.2–77 K) in crystals of nitrates or other compounds doped with traces of NO_2 (Atkins and Symons, 1967; Ayscough, 1967; Wertz and Bolton, 1972). In general, these radicals are not stable after the temperature is

raised above 77 K. The high $T_A = 873 \text{ K}$ of NO_2 indicates a crystal lattice stabilization of the radical. As with the hydrocarbons, the large NO_2 radical (N-O distance 1.19 Å) can reside in the M site of the feldspar structure.

Generally, the free radicals CH_3 , C_2H_5 , and NO_2 are not stable above 200 K in fluids; therefore, they cannot be detected in mineral fluid inclusions. In hyalophane and microcline no intracrystalline fluid inclusions in the C-O-H-N system (e.g., CH_4 , C_2H_6) were detected by micro-Raman spectroscopic analysis. Because of their high thermal stability ($T_A = 573$ – 873 K) and their anisotropic spectra, it is unlikely that the free radicals are located in fluid inclusions or adsorbed at the crystal surface or at intracrystalline cracks. It is generally assumed that T_A for structurally bonded free radicals in minerals is in the range of 473–773 K. O^{1-} and SiO_3^- centers in Table 1, which are free radicals by definition, have similar T_A . Furthermore, in all 34 single crystals of hyalophane and microcline studied, the direction cosines of \mathbf{g} and \mathbf{T} tensors of CH_3 and NO_2 centers are the same, and these values are in good agreement with the data of Matyash et al. (1981, 1982). Moreover, hydrocarbons and NO_2 probably reside at K positions and have T_A in the same range (573–873 K) in which the detectable Na and K self-diffusion in feldspar begins. It can be concluded that the free radicals studied must be fixed in orientation in the crystal structure.

In polycrystalline samples of feldspar from Volhyn pegmatites, Proshko et al. (1987) observed the typical CH_3 spectrum of very high intensity (Figs. 8, 14c, 14d). Based on the interpretation of Matyash et al. (1981, 1982), the spectra were attributed to NH_4^+ , and this feldspar determined as buddingtonite. Pavlishin and Bagmut (1988) investigated 152 samples of potassium feldspar from different zones of 11 pegmatite bodies and surrounding granites. From the intensities of the quartets shown in Figure 8, they concluded an active role for NH_4^+ in the formation and transformation of minerals of the chambered pegmatites and enclosing granites, and they pointed out that the K^+/NH_4^+ ratio of potassium feldspar is an indicator of postmagmatic differentiation of the magmatic material.

Systematic investigations based on many feldspar samples from pegmatite and granite of the Ukrainian Shield showed that in samples that contain methane and ethane, no Fe^{3+} spectra can be detected (Matyash et al., 1981, 1982; Pavlishin, 1983; Proshko et al., 1987; Pavlishin and Bagmut, 1988). Microcline samples from Hagendorf pegmatite also failed to show Fe^{3+} spectra; however, in hydrocarbon-bearing hyalophane, Fe^{3+} centers are present. In the spectra of all hydrocarbon-free feldspars studied so far, Fe^{3+} signals have been observed (cf. Table 1 and references therein). The natural P - T conditions for the substitution of hydrocarbons in the feldspar structure are unknown. Experimental thermodynamic data for fluids in the C-H-O system are known mainly for high P - T conditions (e.g., Woermann and Rosenhauer, 1985, and

references therein). Experimental data for mixing in a multicomponent fluid at geologically important P and T conditions are unavailable. Microthermometric and Raman spectroscopic analyses of methane-bearing aqueous fluid inclusions, primarily in pyroxene, garnet, and quartz of skarn facies, indicated trapping T and P of 628–743 K and 1.4–2.5 kbar for garnet, pyroxene, and amphibole skarn (Gerstner et al., 1989). Similar homogenization temperatures (663–723 K) were reported by Weisbrod (1982) for methane in pegmatitic quartz.

ACKNOWLEDGMENTS

I thank A. Beran (Vienna) for providing the hyalophane samples and initial information about their petrogenesis. F. Knolle (Preussag AG) supplied the crystals of Hagendorf microcline, and H. Wondratschek (Karlsruhe) the samples of Eifel sanidine. E. Horn (Göttingen) is gratefully acknowledged for his micro-Raman spectrometry analysis of the hydrocarbon-bearing microcline and hyalophane crystals, and J. Loevenich (Kernforschungsanlage Jülich GmbH) for γ irradiation of the samples. A. Agel (Marburg) provided valuable assistance with manuscript preparation. This work was financially supported by the Deutsche Forschungsgemeinschaft, grant Pe 406/1-1.

REFERENCES CITED

- Atkins, P.W., and Symons, M.C.R. (1967) The structure of inorganic radicals, 310 p. Elsevier, Amsterdam.
- Ayscough, P.B. (1967) Electron spin resonance in chemistry, 451 p. Methuen, London.
- Barker, D.S. (1964) Ammonium in alkali feldspars. *American Mineralogist*, 49, 851–858.
- Beran, A. (1986) A model of water allocation in alkali feldspar, derived from infrared-spectroscopic investigations. *Physics and Chemistry of Minerals*, 13, 306–310.
- Beran, A., Armstrong, J., and Rossman, G.R. (1992) Infrared and electron microprobe analysis of ammonium ions in hyalophane feldspar. *European Journal of Mineralogy*, 4, 847–850.
- Bershov, L.V. (1970) Atomic hydrogen and methane in some natural minerals. *Geokhimiya*, 10, 1275–1278 (in Russian).
- Bershov, L.V., Marfunin, A.S., Mineeva, R.M., and Nasedkin, V.V. (1983) The stabilizing role of iron in the structure of natural glasses. *Doklady Akademii Nauk SSSR*, 268, 960–963 (in Russian).
- Bersohn, M., and Baird, J.C. (1966) An introduction to electron paramagnetic resonance, 274 p. Benjamin, New York.
- Bertelmann, D., Förtsch, E., and Wondratschek, H. (1985) Zum Temperaturverhalten von Sanidinen: Die Ausnahmeholle der Eifel-Sanidin-Megakristalle. *Neues Jahrbuch für Mineralogie Abhandlungen*, 152, 123–141.
- Bljumenfeld, L.A., Wojewodski, W.W., and Semjonow, A.G. (1966) Die Anwendung der paramagnetischen Elektronenresonanz in der Chemie, 308 p. Akademische Verlagsgesellschaft, Frankfurt, Germany.
- Borutskiy, B.E., Organova, H.I., Marsii, I.M., Simonov, M.A., and Sheslesin, E.P. (1984) Crystal structure and Si,Al disorder of adularia and microcline from Hybin. *Istvestiya Akademii Nauk, SSR, Serya geologicheskaya*, 12, 96–103 (in Russian).
- Carrington, A., and McLachlan, A.D. (1967) Introduction to magnetic resonance, 266 p. Harper, New York.
- Edgar, A., and Vance, E.R. (1977) Electron paramagnetic resonance, optical absorption, and magnetic circular dichroism studies of the CO_3^- molecular-ion in irradiated natural beryl. *Physics and Chemistry of Minerals*, 1, 165–178.
- Fessenden, R.W., and Schuler, R.H. (1963) Electron spin resonance studies of transient alkyl radicals. *Journal of Chemical Physics*, 39, 2147–2195.
- Gaite, J.M., and Michoulier, J. (1970) Application de la résonance paramagnétique électronique de l'ion Fe^{3+} à l'étude de la structure des feldspaths. *Bulletin de la Société Française de Minéralogie et de Cristallographie*, 93, 341–356.
- Gerstner, M.R., Bowman, J.R., and Basteris, J.D. (1989) Skarn formation at the Macmillan Pass tungsten deposit (Mactung), Yukon and Northwest Territories. I. P - T - X - V characterization of the methane-bearing, skarn-forming fluids. *Canadian Mineralogist*, 27, 545–563.
- Gimarc, B.M. (1979) Molecular structure and bonding. Academic, 224 p. New York.
- Höchli, U. (1964) Electron spin resonance of Fe^{3+} in feldspar. In R. Servant, and A. Charru, Eds., *Proceedings of the XIIth Colloque Ampère, Bordeaux 17–21 September 1963*, p. 191–197.
- Hofmeister, A.M., and Rossman, G.R. (1985) A model for the irradiative coloration of smoky feldspar and the inhibiting influence of water. *Physics and Chemistry of Minerals*, 12, 324–332.
- Ikeya, M., Devine, S.D., Whitehead, N.E., and Hedenquist, J.W. (1986) Detection of methane in geothermal quartz by ESR. *Chemical Geology*, 56, 185–192.
- Jen, C.K., Foner, S.N., Cochran, E.L., and Bowers, V.A. (1958) Electron spin resonance of atomic and molecular free radicals trapped at liquid helium temperature. *Physical Review*, 112, 1169–1182.
- Joffe, V.A., and Yanchevskaya, I.S. (1968) Electron paramagnetic resonance and thermoluminescence of irradiated single crystals of the aluminosilicates $\text{NaAlSi}_3\text{O}_8$ and LiAlSiO_4 . *Soviet Physics, Solid State*, 10, 2, 370–374.
- Joppin, G.R., and Willard, J.E. (1972) Further studies of chemical reactions on c-irradiated silica gel and porous Vycor glass. *Journal of Physical Chemistry*, 76, 3158–3166.
- Kimball, M.R., and Megaw, H.D. (1972) Interim report on the crystal structure of buddingtonite. In W.S. MacKenzie and J. Zussman, Eds., *The feldspars: Proceedings of NATO Advanced Study Institute, Manchester 11–21 July 1972*, p. 81–86. Manchester University Press, Manchester, U.K.
- Kroll, H., and Ribbe, P.H. (1983) Lattice parameters, composition, and Al,Si order in alkali feldspars. In *Mineralogical Society of America Reviews in Mineralogy*, 57–99.
- Loewenstein, W. (1954) The distribution of aluminium in the tetrahedra of silicates and aluminates. *American Mineralogist*, 39, 92–96.
- Mackey, J.H. (1963) EPR study of impurity-related color centers in germanium doped-quartz. *Journal of Chemical Physics*, 39, 74–83.
- Marfunin, A.S., and Bershov, L.V. (1970) Paramagnetic centers in feldspar and their possible crystallochemical and petrological significance. *Doklady Akademii Nauk SSSR*, 193, 412–414, 1970).
- Marfunin, A.S., and Michoulier, J. (1966) Résonance paramagnétique électronique de l'ion Fe^{3+} dans un monocristal d'oligoclase. *Comptes Rendus de l'Académie des Sciences de Paris*, 262, 1543–1546.
- Marfunin, A.S., Bershov, L.V., Meilman, M.L., and Michoulier, J. (1967) Paramagnetic resonance of Fe^{3+} in some feldspars. *Schweizerische Mineralogische und Petrologische Mitteilungen*, 47, 13–20.
- Matyash, I.V., Brik, A.B., Zayak, A.P., and Masykin, V.V. (1981) Radiospectroscopy of feldspar, 112 p. *Naukova Dumka, Kiev* (in Russian).
- Matyash, I.V., Bagmut, N.N., Litovchenko, A.S., and Proshko, V.Ya. (1982) Electron paramagnetic resonance study of new paramagnetic centers in microcline-perthites from pegmatites. *Physics and Chemistry of Minerals*, 8, 149–152.
- Matyash, I.V., Brik, A.B., Zayak, A.P., and Masykin, V.V. (1987) Radiospectroscopy of quartz, 167 p. *Naukova Dumka, Kiev* (in Russian).
- Megaw, H.D. (1956) Notation for feldspar structures. *Acta Crystallographica*, 9, 56–60.
- Michoulier, J., and Gaite, J.M. (1972) Site assignment of Fe^{3+} in low symmetry crystals. Application to $\text{NaAlSi}_3\text{O}_8$. *Journal of Chemical Physics*, 56, 5205–5213.
- Morton, J.R., and Preston, K.F. (1978) Atomic parameters for paramagnetic resonance data. *Journal of Magnetic Resonance*, 30, 577–582.
- Niebuhr, H.H., Zeira, S., and Hafner, S.S. (1973) Ferric iron in plagioclase crystals from anorthosite 15415. *Geochimica et Cosmochimica Acta*, 1, 971–982.
- Noble, G.A., Serway, R.A., Donnell, A.O., and Freeman, E.S. (1967) Stability of methyl radical trapped in zeolite matrix. *Journal of Physical Chemistry*, 71, 4326–4329.
- Pavlishin, V.I. (1983) In *Typomorphismus der Quarze, Glimmer und*

- Feldspäte in endogenen Bildungen, 232 p. Naukova Dumka, Kiev (in Russian).
- Pavlishin, V.I., and Bagmut, H.H. (1988) NH_2^+ in pegmatitic and granitic feldspar. *Mineralogicheskii Zhurnal*, 10, 69–71 (in Russian).
- Petrov, I. (1985) Paramagnetische Elektronenspinresonanz von Fe^{3+} in Sanidin. *Fortschritte der Mineralogie*, 63, 180.
- (1992) Application of EPR spectroscopy in mineralogy, petrology and geology. In Council of Scientific Research Integration, Ed., *Trends in mineralogy*, p. 193–267. India.
- Petrov, I., and Hafner, S.S. (1988) Location of trace Fe^{3+} ions in sanidine, KAlSi_3O_8 . *American Mineralogist*, 73, 97–104.
- Petrov, I., Yude, F., Bershov, L.V., Hafner, S.S., and Kroll, H. (1989a) Order-disorder of Fe^{3+} ions over the tetrahedral positions in albite. *American Mineralogist*, 74, 604–609.
- Petrov, I., Agel, A., and Hafner, S.S. (1989b) Distinct defect centers at oxygen positions in albite. *American Mineralogist*, 74, 1130–1141.
- Petrov, I., Mineeva, R.M., Bershov, L.V., and Agel, A. (1993) EPR of $[\text{Pb-Pb}]^{2+}$ mixed valence pairs in amazonite type microcline. *American Mineralogist*, 78, 500–510.
- Pietrzak, T.M., and Wood, D.E. (1970) EPR study of the hindered motion of NO_2 and ClO , adsorbed in synthetic zeolites. *The Journal of Chemical Physics*, 53, 2454–2459.
- Poole, C.D., Farach, A.H., and Bishop, T.P. (1977) Electron spin resonance of minerals. I. Nonsilicates. *Magnetic Resonance Review*, 4, 137–195.
- Proshko, W.Ya., Bagmut, H.H., Vasilishin, I.S., and Panchenko, W.I. (1987) Ammonium feldspar from Volhyn pegmatite and its radiosopic behaviour. *Mineralogicheskii Zhurnal*, 9, 67–71 (in Russian).
- Ribbe, P.H. (1983) Aluminium-silicon order in feldspars: Domain textures and diffraction patterns. *Mineralogical Society of America Reviews in Mineralogy*, 21–55.
- Scala, C.M., Hutton, D.R., and McLaren, A.C. (1978) NMR and EPR studies of the chemically intermediate plagioclase feldspars. *Physics and Chemistry of Minerals*, 3, 33–44.
- Schnadt, R., and Schneider, J. (1970) The electronic structure of the trapped-hole center in smoky quartz. *Physik der kondensierten Materie*, 11, 19–42.
- Shcherbakova, M.Ya., Sobolev, E.V., Samsonenko, N.D., and Aksenov, V.K. (1969) Electron paramagnetic resonance of ionized nitrogen pairs in diamond. *Soviet Physics, Solid State*, 11, 1104–1106.
- Shcherbakova, M.Ya., Sobolev, E.V., and Nadolinnyi, V.A. (1972) Electronic paramagnetic resonance of low-symmetry impurity centers in diamond. *Soviet Physics Doklady*, 17, 513–516.
- Smith, W.V., Sorokin, P.P., Gelles, I.L., and Lasher, G.J. (1959) Electron-spin resonance of nitrogen donors in diamond. *Physical Review*, 115, 1546–1552.
- Solntzev, V.P. (1981) Color centers and EPR of beryl and chrysoberyl. *Akademie Nauk SSSR, Problemyi theoreticheskoy i geneticheskoy mineralogii*, 499, 92–140 (in Russian).
- Speit, B. (1980) Struktur und Eigenschaften von Farbzentren in Feldspäten. Thesis, University of Münster, Germany.
- Speit, B., and Lehmann, G. (1976) Hole centers in the feldspar sanidine. *Physica Status Solidi*, 36A, 471–481.
- (1982) Radiation defects in feldspars. *Physics and Chemistry of Minerals*, 8, 77–82.
- Suharzhovskyi, S.M. (1976) Structural study of the NO_2 molecule in beryl. *Voprosy Geokhimi i tipomorphism mineralov*, 1, 22–29 (in Russian).
- Weisbrod, A. (1982) Physical and chemical changes in natural fluids in hydrothermal processes and mineral deposition, studied with fluid inclusions. *Berichte der Bunsengesellschaft Physikalische Chemie*, 86, 1016–1027.
- Wertz, J.E., and Bolton, J.R. (1972) *Electron spin resonance: Elementary theory and practical applications*, 497 p. McGraw-Hill, New York.
- Woermann, E., and Rosenhauer, M. (1985) Fluid phases and redox state of the Earth's mantle. *Fortschritte der Mineralogie*, 63, 263–349.

MANUSCRIPT RECEIVED DECEMBER 31, 1992

MANUSCRIPT ACCEPTED NOVEMBER 5, 1993